Structural Integrity 11
Series Editors: José A. F. O. Correia · Abílio M. P. De Jesus

António Arêde
Cristina Costa *Editors*

Proceedings of ARCH 2019

9th International Conference on Arch Bridges

Springer

Structural Integrity

Volume 11

The *Structural Integrity* book series is a high level academic and professional series publishing research on all areas of Structural Integrity. It promotes and expedites the dissemination of new research results and tutorial views in the structural integrity field.

The Series publishes research monographs, professional books, handbooks, edited volumes and textbooks with worldwide distribution to engineers, researchers, educators, professionals and libraries.

Topics of interested include but are not limited to:

- Structural integrity
- Structural durability
- Degradation and conservation of materials and structures
- Dynamic and seismic structural analysis
- Fatigue and fracture of materials and structures
- Risk analysis and safety of materials and structural mechanics
- Fracture Mechanics
- Damage mechanics
- Analytical and numerical simulation of materials and structures
- Computational mechanics
- Structural design methodology
- Experimental methods applied to structural integrity
- Multiaxial fatigue and complex loading effects of materials and structures
- Fatigue corrosion analysis
- Scale effects in the fatigue analysis of materials and structures
- Fatigue structural integrity
- Structural integrity in railway and highway systems
- Sustainable structural design
- Structural loads characterization
- Structural health monitoring
- Adhesives connections integrity
- Rock and soil structural integrity

Springer and the Series Editors welcome book ideas from authors. Potential authors who wish to submit a book proposal should contact Dr. Mayra Castro, Senior Editor, Springer (Heidelberg), e-mail: mayra.castro@springer.com

More information about this series at http://www.springer.com/series/15775

António Arêde · Cristina Costa
Editors

Proceedings of ARCH 2019

9th International Conference on Arch Bridges

Springer

Editors
António Arêde
Faculdade de Engenharia
University of Porto
Porto, Portugal

Cristina Costa
School of Technology,
Department of Engineering
Polytechnic Institute of Tomar
Tomar, Portugal

ISSN 2522-560X ISSN 2522-5618 (electronic)
Structural Integrity
ISBN 978-3-030-29226-3 ISBN 978-3-030-29227-0 (eBook)
https://doi.org/10.1007/978-3-030-29227-0

This Springer imprint is published by the registered company Springer Nature Switzerland AG
The registered company address is: Gewerbestrasse 11, 6330 Cham, Switzerland

Preface

Arch structures, somehow inspired in nature-based forms since remote times, provide examples of remarkable masterpieces of engineering art and skills. In what concerns bridges, arch ones have lasted for centuries to present time in fairly good conservation state and still coexisting with other modern and quite different bridge typologies. By exploring the stable compression state of materials, arch bridges clearly remain competitive as evidenced by recent examples near 400-m span built under highly demanding requirements.

Arch bridges' science and technology therefore persist as a key issue in engineering as shown by the high-quality and successful eight previous international conferences on arch bridges held in UK 1995, Italy 1998, France 2001, Spain 2004, Portugal 2007, China 2010, Croatia 2013, and Poland 2016.

Stemming from such heritage, the 9th International Conference on Arch Bridges (ARCH 2019) is held in Porto, Portugal, during October 2–4, 2019, organized the Faculty of Engineering of the University of Porto. This conference provides an international forum for all those who deal with arch bridge structures, namely scientists, designers, technicians, stakeholders, and contractors, seeking for related knowledge, experience, and specialized information exchange and diffusion.

The conference addresses key topics related to arch bridges, such as historical, analytical, numerical, and experimental investigations, design and construction, rehabilitation, maintenance and condition assessment, and future trends. Three special sessions were organized and included in the program, focusing on "Experimental and numerical assessment," "Design and Construction," and "Structural rehabilitation and maintenance."

Full contributions presented in ARCH 2019, including five invited keynote papers and 99 research and technical papers, were prepared by authors from 26 countries and are assembled in the conference proceedings published in this volume of the Springer Structural Integrity book series. Papers are distributed in six parts covering the following topics: (i) heritage arch bridges; (ii) analytic and numerical studies of arch structures; (iii) analytic and numerical studies of arch structures; (iv) design and construction of arch bridges; (v) rehabilitation, maintenance, and condition assessment of arch bridges, and (vi) new and future trends in arch bridges.

The organizing committee of ARCH 2019 expresses a special acknowledgment to all participants and authors for their valuable contributions for this book series, to the special session organizers for their commitment, to the advisory and scientific committee members for their careful work and to all sponsors for their institutional and financial support. Also, the Springer is fully acknowledged for the support to the Structural Integrity book series.

October 2019

António Arêde
Cristina Costa

Sponsors

Conference Organization

U.PORTO
FEUP FACULDADE DE ENGENHARIA
UNIVERSIDADE DO PORTO

CONSTRUCT

INSTITUTO DA CONSTRUÇÃO

Silver Sponsors

CONDURIL

PRETENSA

AP Bridge Construction Systems Portugal, Lda

Bronze Sponsors

RUBRICA BRIDGES

A CONSTRUIR CONFIANÇA Sika

AOF augusto de oliveira ferreira & ca lda

A400 PROJETISTAS E CONSULTORES DE ENGENHARIA

Azvi Portugal

Other Sponsors

UNIÃO EUROPEIA
Fundo Europeu
de Desenvolvimento Regional

Contents

Design and Construction of Arch Bridges

Keynote Lectures

Masonry Bridges and Viaducts: Testing, Mechanics, Retrofitting Towards an Extended Life

Antonio Brencich(✉)

Polytechnic School, University of Genoa, via Montallegro 1, 16145 Genoa, Italy
brencich@dicca.unige.it

Abstract. Due to the large number of masonry bridges in the European Infrastructural network, the maintenance and retrofitting of this kind of bridges is an up-to-date issue of Structural Engineering. In this paper, the Mechanics of masonry bridges is discussed starting from the definition of load carrying structure, which is much wider than the arch itself. Once proper similarity criteria for reduced scale laboratory testing are discussed, the results of some tests are used to outline the basic features of the mechanical response of masonry bridges. Arch-Fill interaction turns out to be crucial for the l.c.c. of the bridge since it is responsible also for the span of the structural arch. The concept of Limit Load is discussed, which is not so trivial to be defined as usually assumed since it does not correspond to the Ultimate Load that activates a collapse mechanism. Once the basic issues of the dynamic and seismic response of masonry bridges are discussed, showing unexpected good seismic performances of these massive bridges, new trends in retrofitting of the bridges are discussed.

Keywords: Masonry bridge · Load carrying structure · Retrofitting

1 Introduction

Masonry bridges play a crucial role in the railway and road networks of the European Union, where they are estimated to be something in-between 200.000 and 250.000, and in the railway and road networks of many other countries, such as India and Japan. The age of these bridges, accounting for degradation of the materials, the past and present changes in the service standards (speed and load) and the reduced, if any, maintenance put forward the importance of assessing and retrofitting this kind of bridges. Their mechanical response were not completely understood till the scientific and technical research of the last three decades explained the basic aspects of their structural response. The I/03/U/285 Research Project by the International Railway Union (UIC) and the E.U. Sustainable Bridges Project (6^{th} Framework Program, project 1653) are two relevant examples [1, 2].

The scientific research was reactivated by some tests on reduced scale bridge models studying the mechanics and the collapse of masonry bridges [3–5]. These tests showed that the collapse of a masonry arch bridge could be activated by a 4 hinge

A. Arêde and C. Costa (Eds.): ARCH 2019, SI 11, pp. 3–30, 2020.
https://doi.org/10.1007/978-3-030-29227-0_1

mechanism, apparently corroborating the Kinematic Approach discussed by Heymann [6]. Unluckily, the tests were biased by the reduced scale of the samples: since no similarity criterion was set, reduction of the geometric scale only made the model-to-prototype similarity to be lost. If the model-to-prototype similarity is retained [7], either increasing the gravity loads (tests performed in centrifuge) [5] and reducing the compressive strength for masonry [8], the outcomes of the tests show that brickwork crushing may play a crucial role in the collapse of a masonry bridge, which is significantly different from a pure Kinematic Approach.

In spite of the recent outcomes of scientific research, some approaches are still used in professional Engineering, such as the MEXE-MOT method [9], proposed in the '60s, assuming that the limit load of single and multi-span bridges can be deduced from the load carrying capacity of the arch barrel only. Some important parameters, such as masonry strength, mechanical characteristics of the fill, span interaction, pier stiffness, etc., are taken into account by means of corrective factors of uncertain origin [10].

More recent approaches estimate of the load carrying capacity of arches based on the Static (safe) and Kinematic Theorems of Limit Analysis. Assuming brickwork as a No Tensile Resistant material, a non linear constitutive model in compression for brickwork is needed to represent the response of a bridge, till the ultimate load, by means an incremental step-wise analysis in which convergence to the solution is reached through an iterative procedure. The Mechanism Approach, derived from the Kinematic Theorem, instead, assumes a compressive brittle behavior (with unbounded or finite compressive strength) and sets collapse in advance as the activation of a number of point-like hinges in the arch is large enough to turn the arch into a mechanism.

The kinematic approach gives reasonable estimates of the limit load when the collapse mechanism is activated at relatively low stress levels, i.e. for deep arches, for which the non linear response of brickwork plays a minor role. When this is not so, i.e. for shallow bridges, this approach seems to be somehow troublesome and a step-wise incremental procedure has to be set. In this latter case, more accurate iterative schemes and more detailed 1-D [11–16], 2-D [17–21 among the latest results] and 3-D models [22–25 as some of the most recent examples] are needed to represent the mechanical response of the bridge. Due to the large computational power that can be easily accessed nowadays, non linear computational procedures are nowadays the tool for studying a masonry bridge.

The analysis of post-seismic damage shows that these massive bridges show limited damage, mainly related to local collapse mechanisms (overturning of the spandrels), while the global collapse of the bridges is seldom recorded but for some specific case. The dynamic tests, that are still far from giving a comprehensive understanding of the dynamic response of masonry bridges, show that these structures have large damping values, probably due to the frictional interfaces of the bridge (arch-fill and spandrel-fill) and to the damping of the fill itself.

In this paper, the mechanical response of masonry bridges is discussed aiming at the assessment and retrofitting of this kind of structures. In situ and laboratory tests and theoretical results show that masonry bridges are complex structures in which all the elements play a role in the load carrying capacity. Thus, assessing and retrofitting of a bridge should take into account a complete model of the bridge looking into the inner

mechanics of the structure. The assessment and retrofitting strategies are then discussed addressing either some of the common retrofitting technique and the new trends.

2 Statistics

Table 1 and Fig. 1 give a summary of the in-service railway bridge stock in E.U. [26]. Even though 50% of the bridge stock is less than 2 m long, i.e. a kind of culvert, it is evident the large number of masonry bridges and that 15% of the stock, at least, needs assessing and some kind of retrofitting.

Table 1. Railway bridges in Europe [26] – any span.

Country	Total length [km]	Bridges total	Bridges/km	Mas. bridges	%	Oldest bridge
Belgium	3.607	3400	0.9	60	18	1845
U.K. – Br. Rail	15.811	26.240	1.7	13.000	50	**1825**
Bulgaria	4.070	982	0.2	62	6	1867
Denmark	2.560	1500	0.6	135	9	1853
Germany	**41.315**	32.017	0.8	9.146	29	1837
Finland	8.816	1.905	0.4	60	3	1861
France	29.901	28.259	1.0	13.167	47	1840
Greece	2.238	2.100	0.9	710	34	1883
Italy	16.723	**59.473**	**3.7**	**37.400**	**63**	1850
Ireland	2.733	2.752	1.0	1.484	54	1839
Luxemburg	274	282	1.0	149	53	1859

3 Laboratory and in Situ Tests

In order to retain the similarity of the tested model to the real prototype, we can recall the Buckingam Theorem [27]. In general, the load carrying capacity P_u can be assumed to depend on: (i) material compressive strength f_M; (ii) arch span l; (iii) material density ρ; (iv) the thickness s of the arch, the width w of the arch barrel, the thickness t of the fill in crown and other geometrical parameters a_i:

$$P_u = g(f_M, l, \rho, s, t, w, a_i) \tag{1}$$

Assuming l and ρ as governing parameters, indicating the physical dimensions of the parameters in square brackets, the following dimensional equation holds:

$$[f_M] = \mathrm{F/L^2} = [\rho][l]. \tag{2}$$

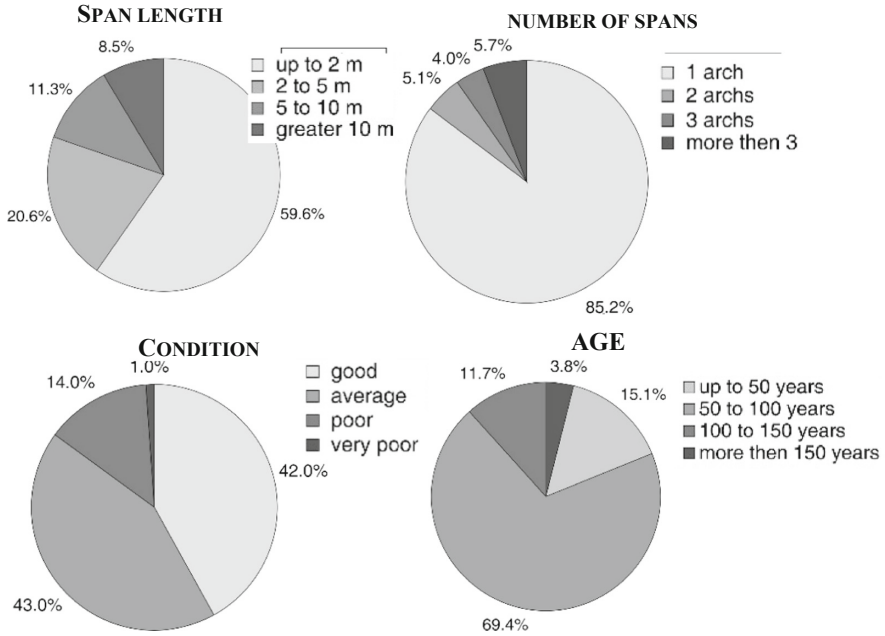

Fig. 1. Statistics of the European Bridge Stock [26] – any span.

If we say α the geometric model-to-prototype ratio, β the compressive strength and γ the density m-to-p ratios, Eq. (2) shows that the similarity criterion may be set as:

$$\alpha\gamma/\beta = const. \tag{3}$$

Equation (3) shows that the similarity of the model to the prototype bridge is retained if the material strength of the model is reduced by the same amount as the geometric ratio. Otherwise, if the material strength is kept constant, the material density may be increased by a factor α as in a centrifuge [5].

If the model is given a 1:α geometric ratio and the materials are the same as for the real prototype (β = 1 and γ = 1) Eq. (3) may not be satisfied. The model-to-prototype similarity is lost: the test results can be extended to a prototype which material has an increased strength (or density) of a factor α. This explains why several tests on reduced scale models showed that the collapse of an arch is due to the activation of a collapse mechanism and not to a compressive crushing of some sections. The tests performed at Bolton Institute [3, 4] used modern engineering bricks for solid clay brickwork obtaining a compressive strength of 26 MPa on the average. Since the geometric ratio of the Bolton tests was approx. 1:4 ÷ 1:3, the similar prototype bridge should have brickwork with a compressive strength of 26 MPa × 3÷4 = 78–104 MPa, which is surely not typical of bridge brickwork [28] and explains why those tests showed that the material strength had a minor role in the collapse mechanics. Similar conclusions can be derived also for other reduced scale tests.

In order to retain the model-to-prototype similarity, we can use for the arch a different material than brickwork scaled by the same factor as the geometric ratio [7] and with the same overall response as brickwork. This is the case of Aerated Autoclaved Concrete, as Fig. 2 shows, which is characterized by f_c = 3 MPA and E = 500 MPa, i.e. a strength and stiffness ratio 1:4 with respect to solid clay brickwork. Since a.a.c. has a reduced density (6.4 kN/m^3), we need to take into account the global mass when calculating the real scale ratio of the model. Besides, only non-cohesive materials can be used for the fill since the friction coefficient is non-dimensional and is not affected by the similarity criterion. A cohesive material, instead, would ask also cohesion to be scaled, which is a rather challenging task.

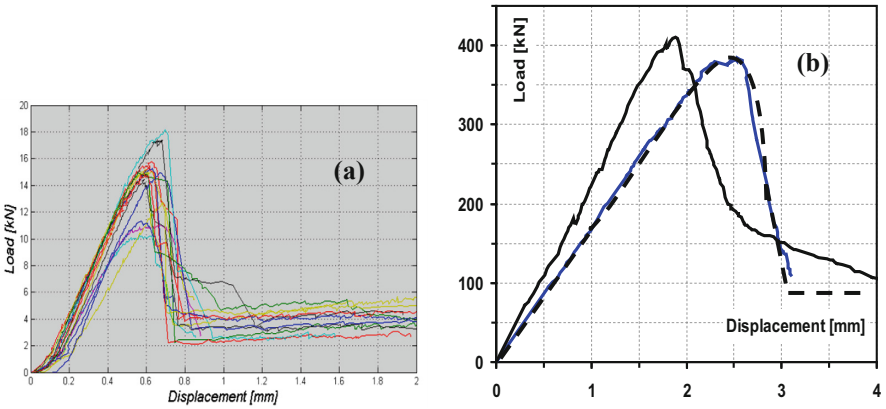

Fig. 2. Compressive response of: (a) aerated autoclaved concrete; (b) bridge brickwork, both showing a Kent&Park type compressive response (dotted line in b).

To discuss the mechanical response of a masonry bridge let us consider the arch of Fig. 3, where rise-to-span ratio *r/s* = 0.2 (spandrels and fill are not represented). Four models have been tested: (i) arch only; (ii) arch + fill + load applied directly on the arch, Fig. 3b; (iii) arch + fill + load applied on the fill, on a 20 cm wide strip; (iv) arch + spandrel (10 cm thick). The fill used in the tests consists of a non-cohesive granular material graded 8–10 mm (internal friction angle: 32°). The arches were an assemblage of pre-cut blocks with no mortar: so that a perfectly No-Tensile-Resistant material has been represented with compressive strength and behavior as in Fig. 2.

Figure 4 shows that the load carrying capacity of an arch accounts for approx. 9% of the l.c.c. of a complete bridge model, while comparison of the two models with fill (load on the arch, Fig. 3b, and load on the fill surface) shows that the fill contributes for load distribution effect of the fill accounts for 70% of the global l.c.c. while the distribution effect of the fill for the remaining 21%. Similar results were obtained on the basis of experimental data by [29] and theoretically by [21].

Figures 5 and 6 show that the collapse mechanism at maximum load shows two hinges only, while the remaining expected two hinges are not activated because the compressive crushing of the material precedes the activation of the other two hinges.

A four hinges mechanism is activated for deep arches, say with rise-to-span ratio = 0.3 [30].

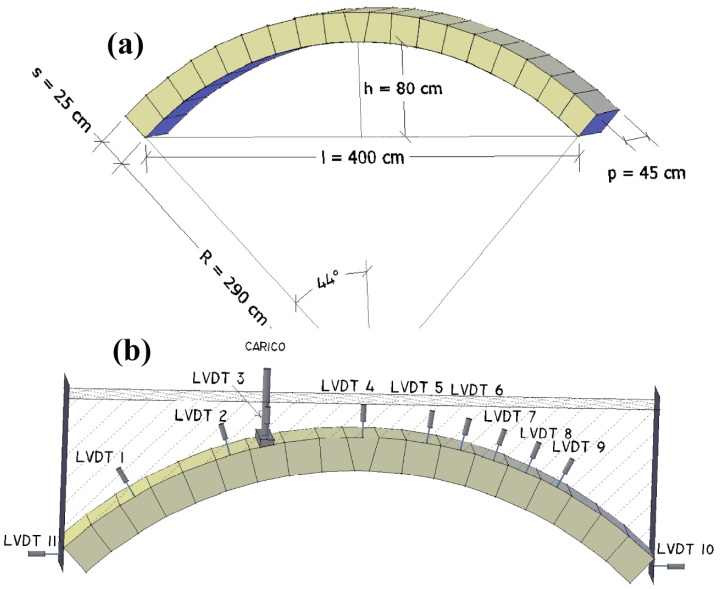

Fig. 3. (a) Arch model. Span 4.00 m, Thickness 25 cm, Width 45 cm, Rise: 80 cm => r/s = 0.2. (b) Experimental setup and loading directly on the arch (case ii)

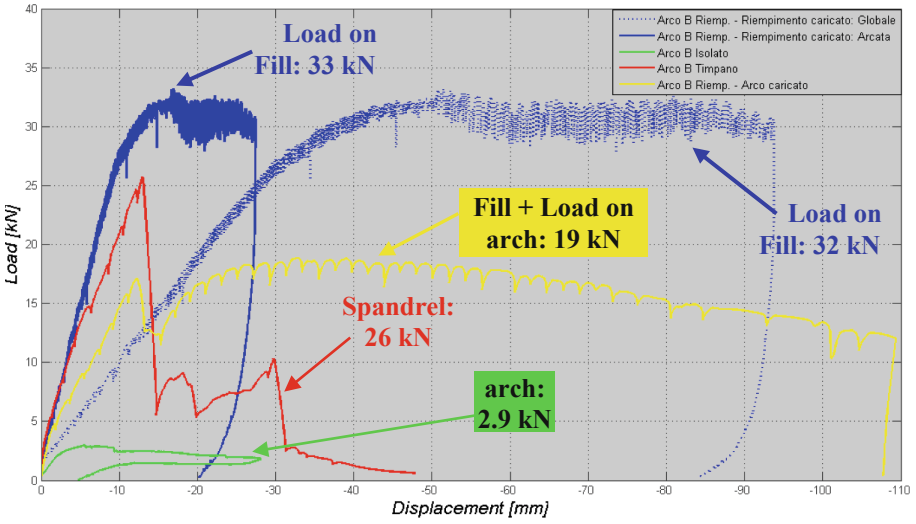

Fig. 4. Load-displacement response of the shallow arch bridge of Fig. 3. Green line: bare arch, Red line: Arch + Spandrel, Yellow line: Arch + Fill and Load directly on the fill, Blue lines: Arch + Fill and Load on the fill surface

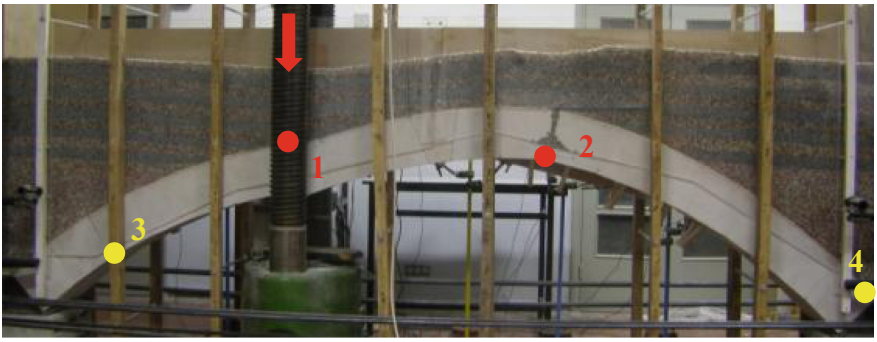

Fig. 5. Collapse mechanism of the arch of Fig. 3, Load applied on the Fill surface. Hinges 1 and 2 were identified (see Fig. 6) and the expected hinges 3 and 4 were not identified.

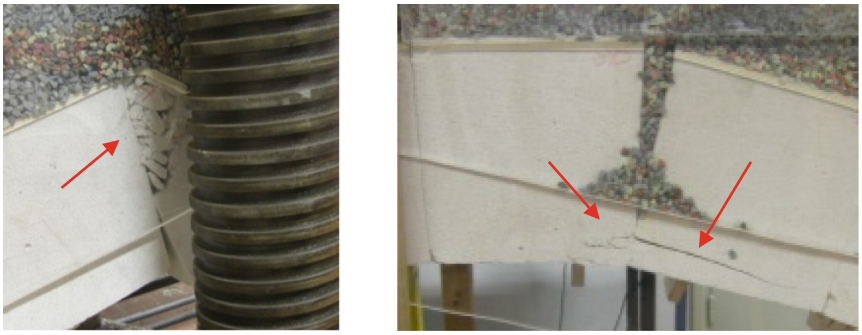

Fig. 6. Detail of hinges 1 (left) and 2 (right) of Fig. 5 showing compressive crushing

Fig. 7. Collapse of a span of a railway multi-span bridge

4 The Load Carrying Structure of a Masonry Bridge

Figure 7 shows the collapsed span of a multi-span railway viaduct. As always happens when the pier survives to the collapse of a single span, we can observe that a large part of the arch from the geometrical springing did not collapse. This shows that the load carrying arch (l.c.a) is much shorter than the geometric arch (g.a.). Figure 8 shows a simple rule to calculate the load carrying arch once the geometry of the backfill is known (from original drawings of the bridge). Table 2 shows a list of large railway Italian multi-span viaducts (design drawings available) for which we can show that the concept of "deep arch" does not apply being the l.c. arch a rather shallow arch instead of the deep arch that is suggested by the external geometry.

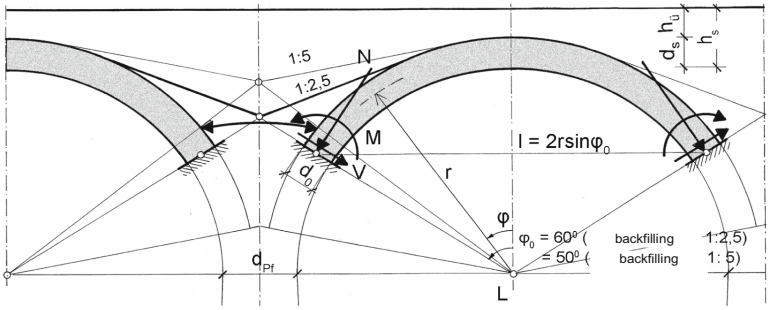

Fig. 8. Actual springing of the arch in a multi-span bridge after Pauser [31]

Table 2. Railway bridges in North-Western Italy apparent and real rise-to-span ratio.

Bridge/ /Viaduct	Line, km / District	spans	Geometric arch			Structural arch		
			s [m]	*r* [m]	*r/s*	*s* [m]	*r* [m]	*r/s*
Traversa	Turin-Genoa, 46.140 / Turin	3	8.0	2.30	0.29	7.0	2.6	0.23
Verde viaduct	Succursale dei Giovi, 8.144 / Genoa	18	18.5	9.25	0.50	14.2*	3.3	0.23
						13.1+	2.8	0.21
Brucoli	Messina-Siracusa, 268.227 / Palermo	3	25.8	12.90	0.50	21.4**	5.8	0.27
Gocciadoro	Mestre-Trento, 143.575 / Trento	75	8.0	4.00	0.50	5.6	1.1	0.20
Mellea	Trofarello-Cuneo, 34.963 / Turin	3	14.1	2.20	0.16	14.1	2.2	0.16
Masserenti	Bologna Circle, 0.461 / Bologna	1	11.4	2.30	0.20	11.4	2.3	0.20
Carsoli	Rome-Sulmona, 77.293 / Rome	4	10.0	5.00	0.50	8.4**	2.1	0.25
Cartecchio	Giulianova-Teramo, 23.669 / Rome	9	20.0	10.00	0.50	17.0	4.7	0.28
Pesio	Fossano-Ceva, 14.200 / Turin	19	25.0	12.50	0.50	21.0	5.3	0.25
Varenna	Genoa-Ovada, 12.918 / Genoa	9	18.5	9.25	0.50	15.5	5.2	0.27
Goriano Sicoli	Rome-Sulmona, 147.886 / Rome	9	10.0	5.00	0.50	8.3	1.9	0.23
Rio Secco	Turin-Modane (Fr), 68.341 / Turin	15	10.0	1.35	0.13	10.0	1.3	0.13
Scrivia	Turin-Genoa, 129.578 / Genoa	1	40.0	13.0	0.32	36.6	7.4	0.20
Tagliata	Turin-Modane (Fr), 54.755 / Turin	1 + 2	30.0	9.5	0.30	27.2	6.1	0.22
Cantalupo	Genoa-Ovada, 13.549 / Genoa	6	18.5	9.25	0.50	15.2	3.9	0.26

s = span *r* = rise *r/s* = rise/span

If we consider that: (i) the load carrying arch in a bridge is always a shallow one, and (ii) the collapse of a shallow arch is attained not due to the activation of a mechanism (4 hinges) but the compressive crushing of the material (2 hinges + crushing in the hinges) we deduce that a kinematic analysis of a masonry bridge does not represent the actual collapse mechanism of the bridge and the ultimate load estimated on the basis of a kinematic approach is a substantial overestimation of the load carrying capacity of the bridge.

5 The Dynamic and Seismic Response

As for any structure, the dynamic identification of a masonry bridge is something rather different from its seismic response because, in the first case, the displacements, either induced by the service loads or by specifically applied forces, remain in the "infinitesimal field" while under seismic actions the expected displacements are much higher.

Figure 9 shows a multi-span railway bridge during demolition that was available for dynamic identification. Its geometry is quite standard but for the fact that it had two internal spandrels at 1/3rd and 2/3rd of the bridge width. Since the arch barrel consisted of 3 parallel barrels, Fig. 10, the internal spandrels where just on the interface between adjacent barrels.

Fig. 9. Multi-span railway bridge on the Tanaro, Alessandria (IT) during demolition.

Fig. 10. Bridge of Fig. 9: the arch consisted of 3 parallel arches connected by transversal ties.

The bridge has been tested [32] in two configurations: with internal spandrels and without internal spandrels. The acting force was a rope pulled by an excavator till it breaks (3.5 kN) in several different locations. Table 3 summarizes frequencies and damping ratios of the first 4 natural modes for the two geometries that were tested and Fig. 11 shows two natural modes (1^{st} and 3^{rd}) as reassembled from the acceleration measurements.

We can see that the arch barrel, either with and without internal spandrels, exhibits rather high damping ratios probably due to the friction between adjacent barrels and to the high damping value of masonry itself. For the complete bridge we could expect similar values since the fill and the other frictional surfaces (fil-spandrel and fill-barrel interfaces) could account for higher damping ratios.

Table 3. First 4 natural frequencies and damping ratios for the bridge of Fig. 9.

Mode	WITH internal spandresl		WITHOUT internal spandrels	
	Freq. [Hz]	Damping ζ	Freq. [Hz]	Damping ζ
1	8.02	9.8	7.07	9.4
2	12.03	6.5	10.90	11.3
3	17.08	7.7	15.09	9.0
4	21.18	3.1	19.34	5.5

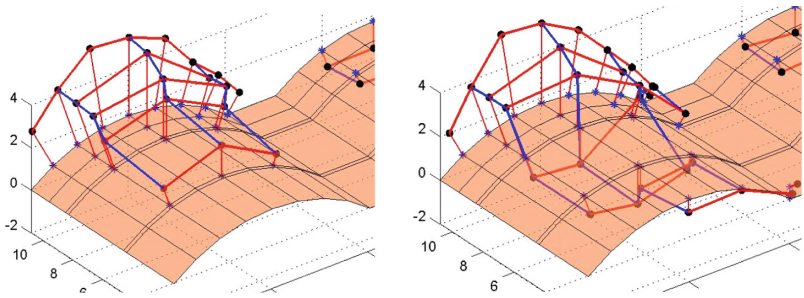

Fig. 11. 1st (8.02 Hz) and 3rd (17.08) natural modes – one span only.

Fig. 12. Seismic damage to a road bridge in Preci (IT) 1997 earthquake (L. Gambarotta).

Is the high damping the reason for the general good performance of masonry bridges under seismic actions? Damping could be just a part of the answer since dynamic testing does not experience the much larger displacements induced by an earthquake. As a matter of fact, we know that masonry bridges are seldom damaged by earthquakes; the Irpinia earthquake (IT) in 1980 did not damage any arch bridge so that the railway infrastructure could reopen to service few days after the event just after a quick survey of the bridges.

Recordings from recent earthquakes show that the most common damage to masonry bridges in the transversal direction is not the overturning of the piers, as one could expect, but the overturning of the external spandrels only, Fig. 12. Damages due to the longitudinal response of the bridge are limited to two cases, one in India to a poor masonry bridge and the second in 2010 in Chile, Fig. 13, which is the only documented collapse of a masonry bridges due to longitudinal seismic response. It has to be noted that the longitudinal dynamic response of a bridge to an earthquake is due also to the asynchronous response of the different piers due to different soils types under the foundations and different stiffness of the piers.

Fig. 13. Collapse of a masonry bridge on the Claro river (Chile) due to longitudinal seismic action, 27th of February 2010.

6 Structural Models

A for all structures, also for masonry bridges there is no optimal structural model, since there is a best model for the specific aim of the structural analysis. In general we can look at a bridge from two points of view.

1. Service Limit State: being far from the ultimate conditions either in static and dynamic conditions, the stress state under the service loads is the main concern. If the bridge had been properly designed (as in the majority of the cases) the stress state in masonry is a substantial compressive state, with low tensile stresses limited to small parts of the bridge, which implies that sometimes also elastic models may be used. The only non linear response may come from the reduced tensile strength of the material, so that the most detailed non linear model should take into account a No-Tensile-Resistant model only for the material, being material crushing of minor relevance. Dynamic identification, that is compared to modal analysis of the bridge, needs just an elastic model to be set.
2. Ultimate Limit State: seeking for the ultimate load, all the main non linear sources should be represented, so that also material crushing and crack propagation through a wide part of the bridge should be considered. Limit Analysis and Incremental Stepwise non linear procedures pertain to this approach. While a masonry bridge, as previously discussed, may not fulfill the assumptions for Limit Analysis procedures to be applied, and this is specifically true for kinematic approaches, also Incremental Stepwise analysis needs to know the initial stress state that is unknown depending on the building phases and the subsequent events (settlement of the foundations, material degradation and time-dependent phenomena).

The use of 1-D, 2-D or complete 3-D models, Fig. 14, depends on the detail of the information that is needed and on the mechanical problem that needs to be investigated.

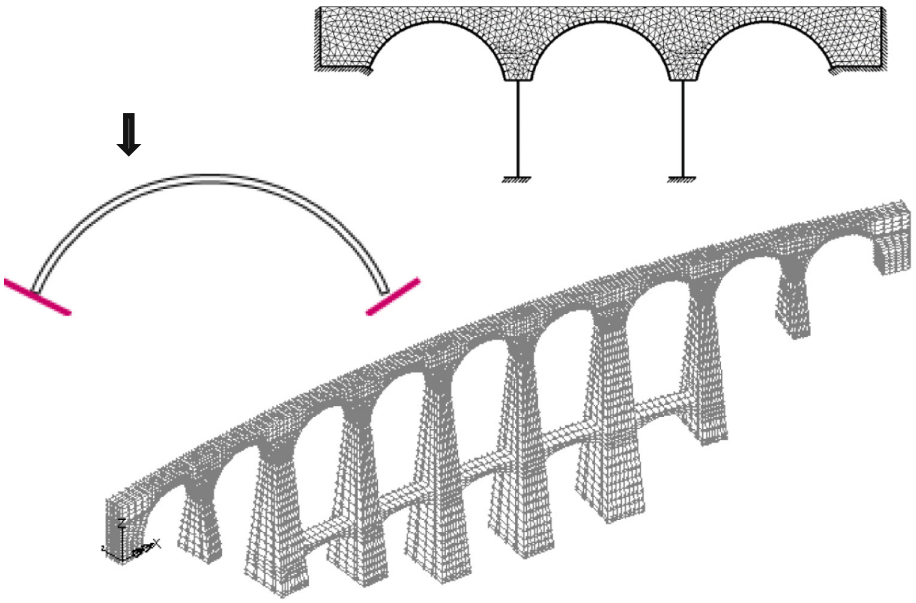

Fig. 14. Structural models for a masonry bridge.

Figure 15 shows a 1-D non-linear model for arches and piers obtained using standard beam elements which are given: (i) No-Tensile-Resistance by means of iterative adaptive meshing following a classical Castigliano scheme; (ii) Elasto-Plastic capabilities obtained adding to an elastic material adding external forces ΔN_{EP} equivalent to the plastic part of the section (red triangle of Fig. 15) [16]. Such an element fits an iterative Predictor-Corrector scheme and allows to study the response of arch-type structures. The effect of the fill and of the external loads is represented by external forces applied to the nodes of the model. Such an approach allows an iterative stepwise procedure to be set, based on the assumption that the only loads on the bridge are the dead loads and the axle load. Any kind of distress due to foundation settlement and/or time dependent (creep of the mortar) or degradation phenomena cannot be considered.

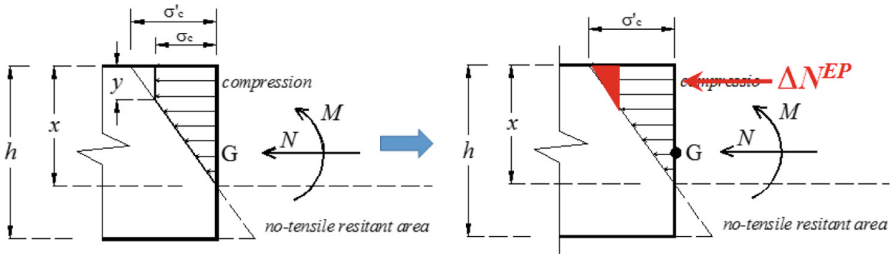

Fig. 15. 1-D model for a No-Tensile-Resistant, Elastic-Perfectly-Plastic model for arch-type structures [16].

Figure 16 shows the model of a three-span bridge, with different rise-to-span ratios, that makes use of the element of Fig. 15. The yellow areas represent the open joints (traction areas) while Fig. 17 shows the Load-Displacement (central crown section) response of the model compared to those of a single arch model. The incremental procedure allows the identification of the load at which the compressive strength of the material is reached (black dots in Fig. 17) and, in a more detailed model, to follow the increase of plastic strains till the material ductility is reached (for solid clay brickwork ductility is limited to 1.4 at maximum). As we can easily see in Fig. 17, in all the models the compressive strength in the first hinge to be activated (i.e. the section below the load) is reached far before the collapse mechanism is activated, being the black dots slightly outside the non-linear part of the diagram. This observation sets a question: which should be the limit load for a real bridge: the one that activates a collapse mechanism (if any, as discussed in Sect. 3) or the load that activates the first permanent strain (and, thus, irrecoverable damage) in some section?

1-D models are those used by the computer programs that makes use of Limit Analysis Approaches, as the well known RING developed at the University of Sheffield [33]. In Fig. 18 the collapse mechanism of a twin-span bridge represented by a RING models is showed. Whatever the width of the bridge, also these models are able of representing the in-plane response of the arch and some of the contributions of the fill.

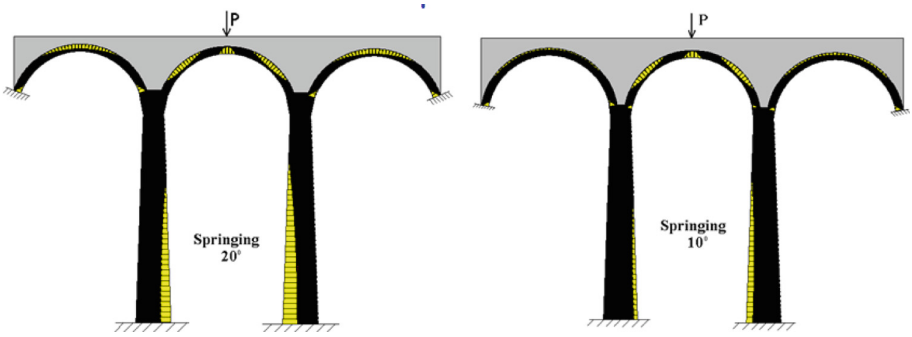

Fig. 16. 1-D models for a 3-span bridge model.

Figure 19 shows a 2-D model for the fill coupled with a beam model for the arch. The No-Tensile-Resistance and Elastic-Perfectly-Plastic response for the arch is represented by the Limit Surface of Fig. 18.b [34].This kind of model allows to take into account the effect of the Arch-Fill interaction, as Fig. 20 shows for a well known case, the Prestwood.

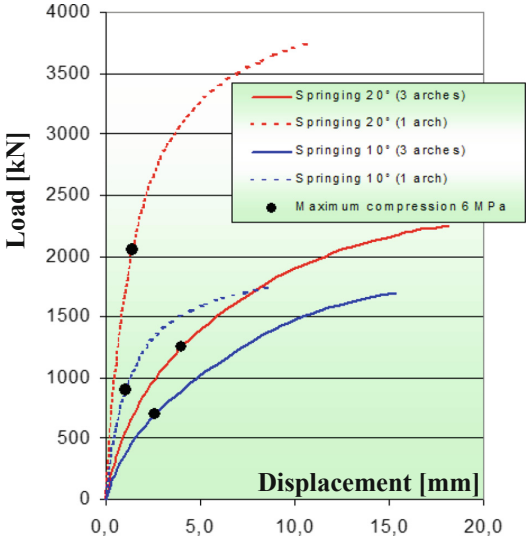

Fig. 17. Load-displacement (crown) of the bridge model of Fig. 16.

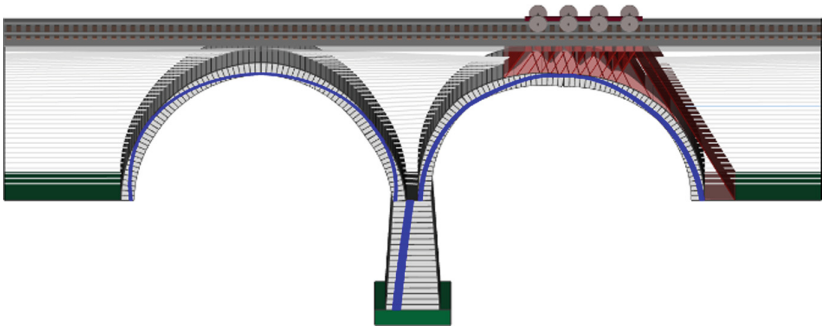

Fig. 18. 1-D model for the collapse of a twin-span bridge following a kinematic approach – from RING 3.0 user's manual [33].

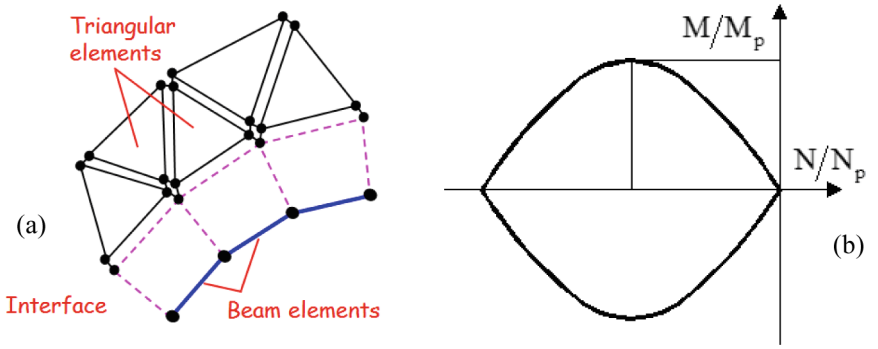

Fig. 19. (a) 2-D model for the fill coupled with beam elements (Fig. 15) for the arch. (b) Elastic-Perfectly-Plastic limit domain for the arch [34].

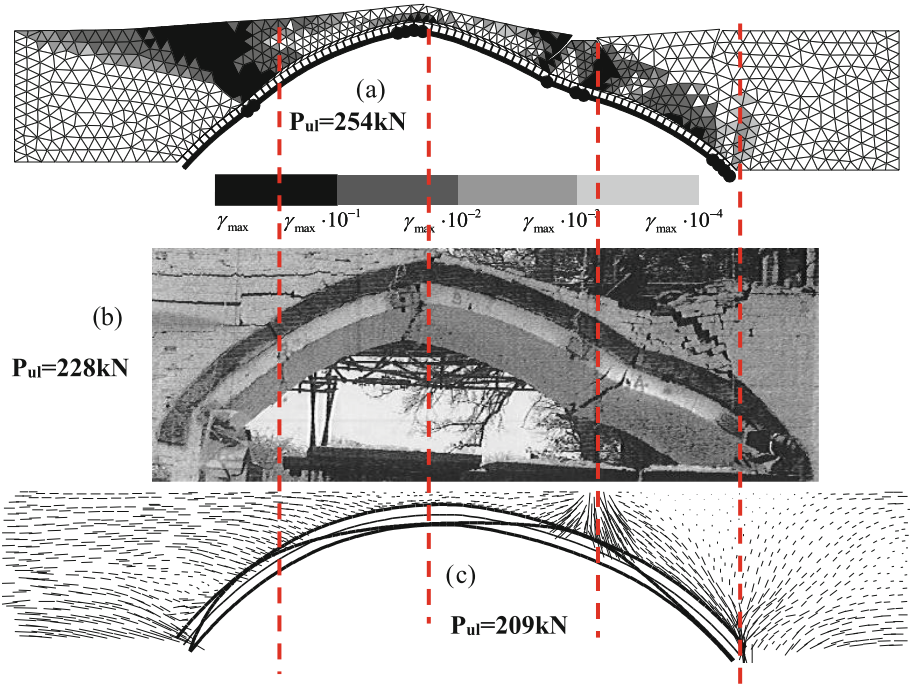

Fig. 20. 2-D model for the Prestwood bridge [35] – comparison with experimental outcomes. (a) 2-D Fem model at ultimate load 254 kN; (b) photo of the collapse 228 kN exp.; (c) Static approach (line of thrust) 209 kN [21, 34].

The 2-D model for the fill allows to represent stresses and strains inside the fill and to represent the fill as a geotechnical structure, i.e. a cohesive soil, Fig. 20, and perform a parametric study on its effect on the ultimate load of the bridge. Looking at the Load-

Displacement diagram of Fig. 21, we note again that the collapse mechanism (4 hinges) is activated far beyond the first plastic strains are activated in the first hinge. For a perfectly brittle material (ductility = 1) the material strength in the arch is attained at a load level that is 2/3rd of the ultimate value, while a ductility set to 2 (rather optimistic for solid clay brickwork) is around 5/6th of the l.c.c. This sets again the basic question on which should be considered the limit load to be used to assess the bridge.

3-D models, which are substantially FEM models only, may provide information on the contribution to the load carrying mechanism of the spandrels and the effect of load eccentricity. The computational effort for the model to be complete is rather high since not only masonry and fill need to be represented but also the frictional interfaces play a crucial role in the bridge response.

If the service conditions need to be investigated, the low stress level and the reduced extension of the tensile stresses, if any, make a simple elastic model to be acceptable. Friction on the interfaces is not activated due to the limited amount of displacements and material non linearity does not play an important role on the stress distribution inside the bridge. For similar reasons, the dynamic characterization of a masonry bridge may be well represented by elastic FEM models due to the reduced displacements of the bridge in the case of service vibrations.

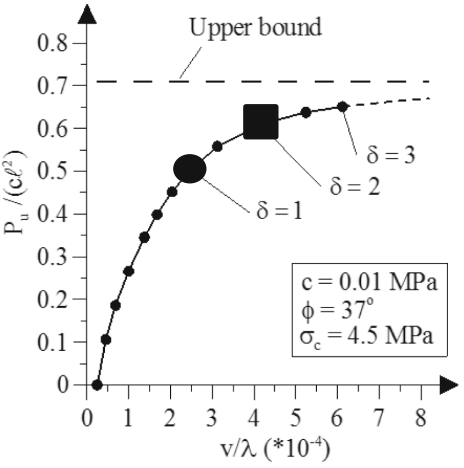

Fig. 21. Load displacement response of the bridge of Fig. 20 [21].

If the ultimate load is the goal of the analysis, then 3-D models have a much worse performance. The frictional interfaces need to be represented and all the non linear features of the material need to be represented, such as No Tensile Resistance and compressive crushing. Whatever the computational power available, the detailed constitutive model for brickwork, the convergence strategy is used, 3-D FEM models fail in a proper representation of the bridge response close to collapse. While the first stage of non linear behavior, i.e. initial cracking of the joints, may be represented, the collapse is characterized by a concentration of cracking, i.e. a diffused cracking in an area turns into a large opening of a specific joint, that FEM models are unable to represent.

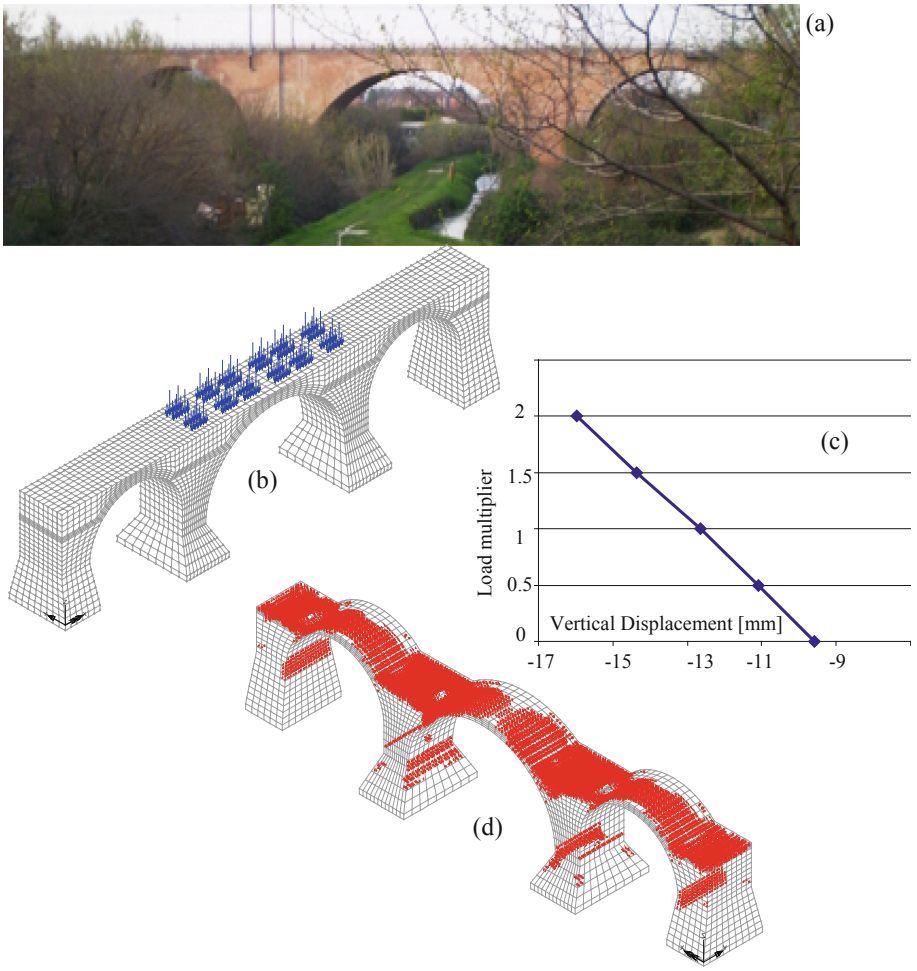

Fig. 22. 3-D FEM model for the Navile Bridge (km 5 + 707 on the Bologna circular line, built 1940 approx.) (a) view of the bridge; (b) 3-D FEM model; (c) load multiplier – displacement response; (d) crack pattern at twice the service loads.

Figure 22 shows the 3-D FEM model of a railway bridge. Figure 22c and d show that non linear response is almost negligible (load-displacement diagram of Fig. 3c) in spite of a rather diffused cracking (Fig. 3d). Convergence is lost at a load multiplier of the max service loads equal to 2 due to the inability of FEM model of representing the concentration of crack opening in specific joints.

7 Retrofitting

Several reasons ask for retrofitting a masonry bridge: degradation of the materials and/or a relevant crack pattern, foundation settlement (if any), increase of the loads, widening of the bridge deck (for road bridges). Due to several historical, technical and cultural reasons, masonry bridges left the classrooms of Engineering Schools not later than the '50s (usually much earlier) leaving space to the up-to-date reinforced concrete and pre-stressed reinforced concrete structures and bridges. As a result, professional engineers need to face a lack of knowledge on masonry bridges that has been integrated, up to recent years, trying to apply the concepts of reinforced concrete to masonry bridges. In the next figures some of the many examples are discussed outlining that the goal of retrofitting a bridge has not usually been achieved and, in many cases, additional damage to the bridge has been produced.

Figure 23 shows a kind of "reinforced masonry". Based on the assumption that the collapse of a bridge takes place due to the activation of a 4 hinge mechanism, near surface reinforcement aims at locking the opening of two of the four hinges. The technique has a crucial problem in the connection to the arch since the curvature tends to detach the reinforcement from the arch as it starts to be active. Besides, it has been discussed that shallow arches collapse due to compressive crushing of some section, so that this retrofitting technique could be of little, if any, help in retrofitting the bridge. When retrofitting a masonry bridge, that is an ancient structure, almost a monument, deserving respect we should always try to preserve the historic value of the bridge. Near surface reinforcement is one of the techniques that makes the value of the monument to be lost.

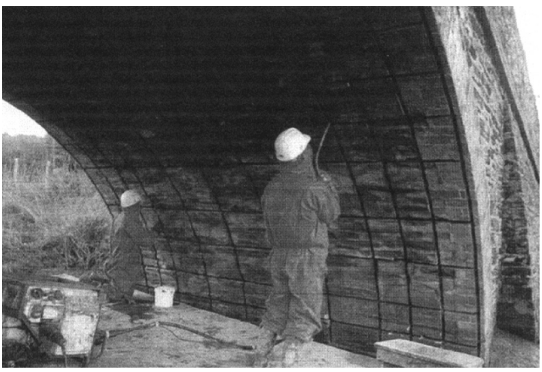

Fig. 23. Connection of stainless steel bars to the arch barrel [36]

Figure 24 shows a rather widely used technique: shotcreting, which motivation is substantially not clear and is usually applied to the existing intrados of the arch ring. If the goal is that of connecting near-surface reinforcement to the arch, its adhesion to brickwork is too poor to be successful in this task. If the goal is that of increasing the thickness of the arch, the different stress state (already compressed the arch, zero

stresses in the added layer) vanish this goal. The only effect is that of encapsulate the bridge in a waterproof skin. Since the water mainly comes into the bridge from above (when the waterproofing systems in no more completely efficient), the outcome is that of speeding up degradation of the material, mainly due to freeze and thaw mechanisms in cold regions, Fig. 24a.

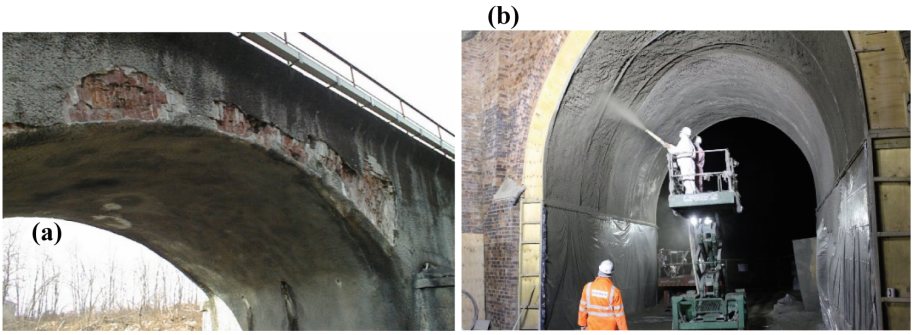

Fig. 24. Shotcreting of a masonry bridge (a) extended to the spandrels; (b) limited to the arch.

Figure 25 shows a typical damage of masonry bridges, i.e. the detachment of the spandrel from the arch barrel, Fig. 25a, that is usually fixed by means of transversal tendons, Fig. 25b. Sometimes, transversal tendons are used also if no damage appears in the barrel in order to provide transversal confinement to the arch. In this latter use, this idea comes directly from the basic knowledge of reinforced concrete but does to apply to the arch since it provides lateral restraint to the arch barrel in one direction only. Besides, it has to be noted that the drills needed to install the tendons produce a damage inside the arch barrel.

Fig. 25. Transversal tie bars from one side of the arch to the opposite side (a) detachment of the spandrel from the arch barrel and (b) *Massarenti Bridge*, Bologna (courtesy RFI).

When widening of the bridge deck is needed, a common technique is that of setting on the deck a r.c. slab supported by the spandrels, Fig. 26; the lateral cantilevers allow the bridge deck to be widened.

This choice reverses the load path from the deck to the bridge. In a masonry bridge the load is applied to the fill and the fill distributes the loads on a wider area on the arch barrel. Such a strategy transfers the loads (also the dead load of the new slab) to the spandrels, which is a loading condition that has never been experienced by the bridge and for which the bridge had never been designed, Fig. 27. The outcome is an overloading of the spandrels and the relief of the arch barrel. Due to compatibility issues, this is responsible of the longitudinal cracks that appear in the arch barrel just below the spandrel (thus underlining the position of the armilla), Fig. 28. The damage produced to the bridge may be severe. In many bridges this kind of damage is facilitated by the fact that the arch is thinner (usually 2/3rds) below the spandrel rather than in its central part [37].

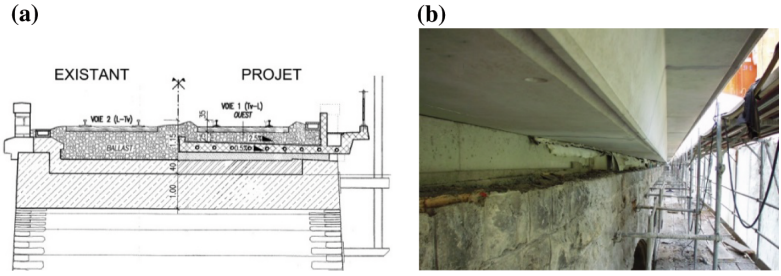

Fig. 26. *Viaduc de Pulvermuhle* (Luxembourg). Widening of the bridge deck by means of an r.c. slab (SNCF, courtesy of B. Plu) (a) design; (b) final slab - view from below

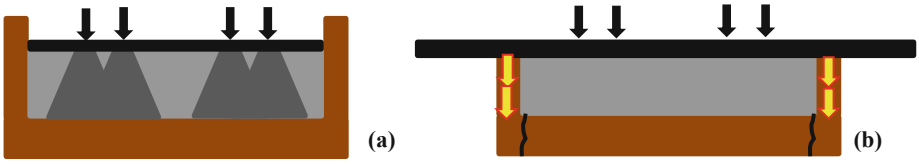

Fig. 27. Load transfer from the deck to the bridge: (a) original arch bridges; (b) case of Fig. 26

Fig. 28. Longitudinal cracks below the spandrel to overloading of the spandrels

Figure 29 shows the effect of a pier on an old bridge. It has to be noted that the collapse pier is inclined with its lower part on the left, i.e. in the downstream part of the river, upstream being on the right as the position of the trunks outlines. It should be noted that the bridge remained undamaged for more than 100 years, during which it experienced several floods, and collapsed in 2002. The reason should be identified in the "protective" collars (reinforced concrete around the pier) that activated the wake effect, Fig. 30, i.e. an increase of excavation not in front of the pier but in its rear side, which is located downstream. This suggests that any kind of "protective collar" (i) should be carefully evaluated since it could reduce the net hydraulic section of the river (in correspondence with the bridge) thus increasing the speed of the flow; (ii) should not be symmetrical with respect to the flow direction in order to move the wake turbulence away from the pier foundation.

In the case of Fig. 29, the wake effect could have been activated/increased by the misalignment between the flow and the pier axis due to a change, in time, of the river longitudinal axis.

Fig. 29. Excavation of a pier - 2002. Note that the base of the pier had been "protected by means of a symmetrical r.c. collar. Bridge on the Scrivia river, District Road 141 – Val Borbera – IT

8 New Trends

In recent years some new approach has been proposed to retrofit masonry bridges preserving their cultural and historical value as much as possible. Figure 31 shows the widening of the deck: an r.c. slab is used but it is detached from the spandrels by means of a layer (soft rubber or foam-rubber) with stiffness that is approx. 100 times less than mortar. In this way, either the dead load of the slab and the live loads are transferred to the fill and not to the spandrels, as in Fig. 29. This allows also to solve another problem, anchoring of safety barriers, that can be easily connected to the slab.

In case of seismic event, the slab represented in Fig. 31 needs some external restraint so as not to rely completely on the bridge, for which it would behave as a relevant mass in its upper part. For this reason, the slab is restrained, with respect to horizontal actions, by large anchorage concrete blocks located outside the bridge at its ends; these blocks are usually connected to vertical and sub-vertical piles to the bedrock, Fig. 31b and c.

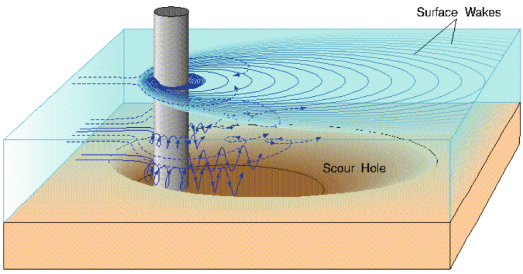

Fig. 30. Wake effect increases the excavation downstream

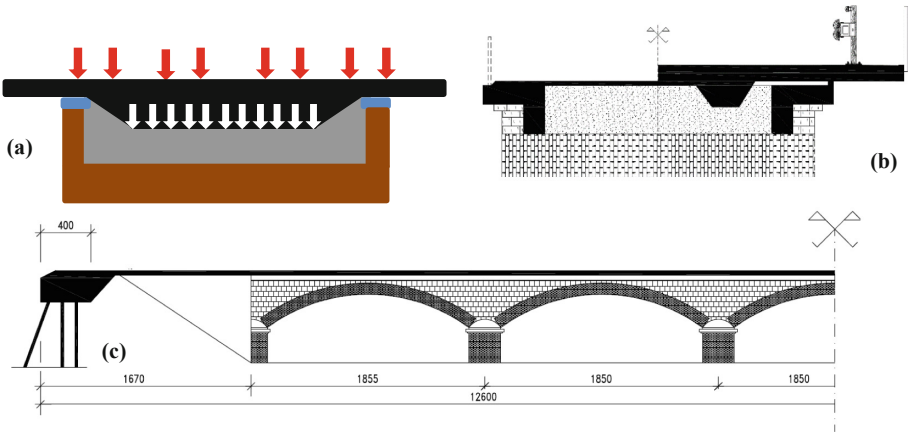

Fig. 31. Reinforced concrete slab enlarging a bridge: (a) load transfer. Bridge on the Borbera river (retrofitting performed in 2014), (b) transversal and; (c) longitudinal section of the slab.

Another technique for increasing the load carrying capacity of a bridge is that represented in Fig. 32: the backfill at springing may be extended injecting the fill. The arch-fil interaction results, in this case, "expected hinges" (if any) would activate at different locations, resulting in a reduced span of the arch. For a multi-span bridge the injection would a large cap at top of the pier and would extend the skewbacks. This technique may be successful for arches with rise-to-span ratio ≈ 0.3, i.e. rather deep arches, as showed in Fig. 33.

Further details of these approaches are discussed in the papers of this Conference.

An alternative approach to masonry bridges aims at increasing their service life strengthening the structure as much as possible also introducing new substitute structures (under-ringing) or deeply modifying the structure and its mechanical response. In this field, it is almost impossible to list all the techniques that have been and are being tested. Some have been discussed in Sect. 7, some of the newest are represented in Figs. 34, 35 and 36 but any listing would be somehow incomplete.

The common approach to these techniques is that they start from the concept of four hinge mechanism (that is activated for deep arches only, as discussed in Sect. 3) and increase the l.c.c. of the arch by locking some of the hinges. Besides, great confidence is given to the effect of drilling piles to strengthen skewbacks, piers and, in general, the foundations. This approach may fit the bridges that are severely damaged by pier scour, material degradation, overloading, etc. since they deeply change the load carrying structure of the bridge, thus loosing a large part of the historical value of the bridge.

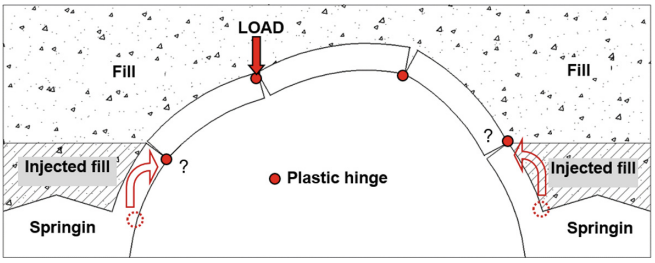

Fig. 32. Uplift of the expected hinge as a result of injecion in the fill

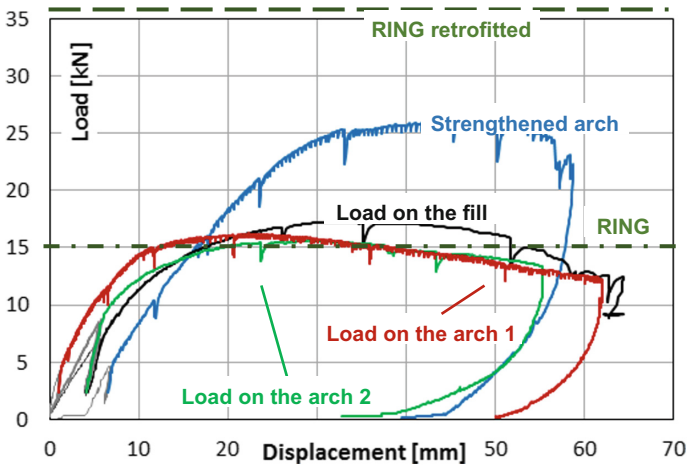

Fig. 33. Load-displacement diagrams for the other models [38] and for the RING model. 4.0 m span model bridge with rise-to-span ratio = 0.3.

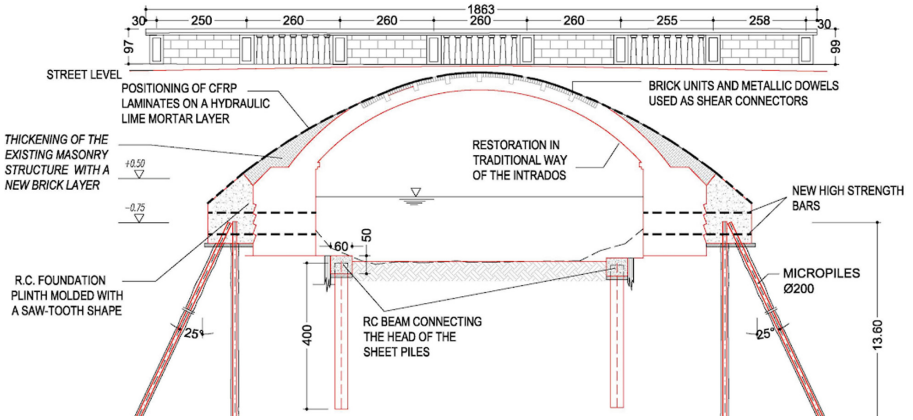

Fig. 34. Deep retrofitting of the *Sandro Gallo* bridge (Venice Lido – Excelsior canal) by extrados reinforcement and piles [39].

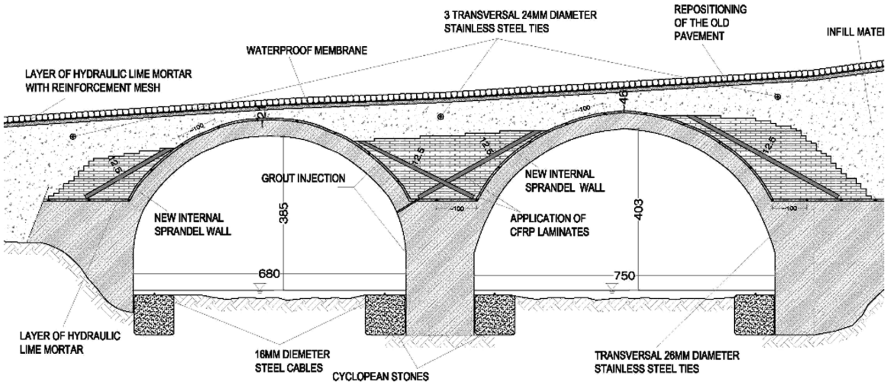

Fig. 35. Deep retrofitting of the *Rio Moline* bridge (Trento – IT) by means of extrados reinforcement and internal tendons [39].

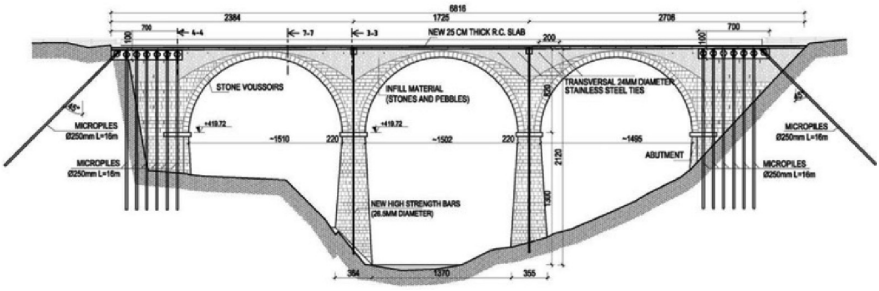

Fig. 36. Deep retrofitting of the bridge over the *Gresal* river (Belluno – IT) by means of pile drilling [39].

9 Conclusions

The large number of masonry bridges on the European transportation network has put forward the need for their maintenance, retrofitting and strengthening with the aim of either keeping them in service and increasing their service life according to the modern performance standards.

It has been discussed that the standard approach to the Mechanics of this kind of bridges deeply relies on the kinematic approach by Heymann [6], i.e. on a collapse mechanism that needs 4 hinges to be activated in an arch (or a larger number in a multi-span bridge). The subsequent retrofitting works aim at locking the activation of some of the hinges.

Other retrofitting procedures just try to apply some of the basic concepts of reinforced concrete to masonry bridges.

These procedures often destroy to a large extent the historical value of a masonry bridge. Their effectiveness is not always guaranteed: the collapse mechanism of a masonry arch bridge may not involve four hinges since the ultimate load may be attained due to compressive crushing of the most stressed sections of the arch. If such a mechanism, that laboratory tests on properly scaled bridge models showed to pertain shallow arches, were activated many of the standard procedures for retrofitting masonry bridges would partially fail in their goal. This is true also for seismic retrofitting, that is a filed of research still in its youth.

Some of the new trends of the last research looks to retrofitting techniques that do not alter the bridge and its historical value, taking into account the actual collapse mechanism.

All these aspects have been discussed and motivated in this paper.

References

1. Orban, Z.: UIC project on assessment, inspection and maintenance of masonry arch railway bridges. In: Lourenço, P., Oliveira, D., Portela, A. (eds.) 5th International Conference on Arch Bridges, ARCH 2007, pp. 3–12. University of Minho, Guimaraes (2007)
2. Sustainable bridges - results from a european integrated research project. In: Bien, J., Elfgren, L., Olofsson, J. (eds.) Dolnoslaskie Wydawnictwo Edukacyjne, Wroclaw, 490 pp. (2007)
3. Melbourne, C., Gilbert, M., Wagstaff, W.: The behavior of multi-span arch bridges. In: Melbrourne, C. (ed.) 1st International Arch Bridge Conference, ARCH 1995, Thomas Telford, London, pp. 489–497 (1995)
4. Melbourne, C., Gilbert, M.: The behavior of multi-ring brickwork arch bridges. The Struct. Eng. **73**, 39–47 (1995)
5. Hughes, T.G., Davies, M.C.R., Taunton, P.R.: Small scale modelling of brickwork arch bridges using a centrifuge. Proc. Inst. Civ. Eng. Struct. Build. **128**(1), 49–58 (1998)
6. Heyman, J.: The Masonry Arch. Ellis Horwood, Chichester (1982)
7. Brencich, A., Riotto G.: Vault-fill interaction on masonry bridges: an experimental approach – 1: statics. In: Bien, J. (ed.) 8th International Conference on Arch Bridges, ARCH 2016, pp. 711–720 (2016)

8. Brencich, A., Cassini, G., Pera, D.: Load bearing structure of masonry bridges. In: Bien, J. (ed.) 8th International Conference on Arch Bridges, ARCH 2016, Wroclaw , pp. 767–774 (2016)
9. Department of Transport: The assessment of highway bridges and structures. (a) Department of Standard BS 21/93, (b) Department of Advice Note BA 16/93 (1993)
10. Harvey, W.: A Guide to the Assessment of Masonry Arch Railway Bridges. UIC (International Railway Union), I/03/U/285 Masonry Arch Bridges Project, Report, July 2007
11. Crisfield, M.A.: A finite element computer program for the analysis of masonry arches. Transport and Road Research Laboratory, Department of Transport, Report LR 1115, TRL, Crowthorne (1984)
12. Crisfield, M.A.: Finite element and mechanism methods for the analysis of masonry and brickwork arches. Transport and Road Research Laboratory, Department of Transport, Research Report 19. TRL, Crowthorne (1985)
13. Bridle, R.J., Hughes, T.G.: An energy method for arch bridge analysis. Proc. Inst. Civ. Eng. **89**, 375–385 (1990)
14. Choo, B.S., Coutie, M.G., Gong, N.G.: Finite-element analysis of masonry arch bridges using tapered elements. Proc. Inst. Civ. Engrs. **91**, 755–770 (1991)
15. Molins, C., Roca, P.: Capacity of masonry arches and spatial frames. J. Struct. Eng. **124**, 653–663 (1998)
16. Brencich, A., De Francesco, U.: Assessment of multi-span masonry arch bridges. Part I: a simplified approach. J. Bridge Eng. ASCE **9**(6), 590–598 (2004)
17. Boothby, T.E., Domalik, D.E., Dalal, V.A.: Service load response of masonry arch bridges. J. Struct. Eng. ASCE **124**(1), 17–23 (1998)
18. Owen, D.R.J., Peric, D., Petrinic, N., Brookes, C.L., James, P.J.: Finite/discrete element models for assessment and repair of masonry structures. In: Sinopoli, A. (ed.) Proceedings of 2nd International Conference on Arch Bridges, Balkema, Rotterdam, pp. 195–204 (1998)
19. Lourenço, P.B., Rots, J.G.: An anisotropic failure criterion for masonry suitable for numerical implementation. Mas. Soc. J. **18**, 11–18 (2000)
20. Fanning, P.J., Boothby, T.E., Roberts, B.J.: Longitudinal and transverse effects in masonry arch assessment. Constr. Build. Mat. **15**, 51–60 (2001)
21. Cavicchi, A., Gambarotta, L.: Collapse analysis of mansory bridges taking into account arch-fill interaction. Eng. Struct. **27**, 605–615 (2005)
22. Fanning, P.J., Sobczak, L., Boothby, T.E., Salomoni, V.: Load testing and model simulations for a stone arch bridge. Bridge Struct.: Ass. Des. Constr. **1**(4), 367–378 (2005)
23. Milani, G., Lourenço, P.B.: 3D non-linear behavior of masonry arch bridges. Comput. Struct. **110**, 133–150 (2012)
24. Costa, C., Ribeiro, D., Jorge, P., Silva, R., Arêde, A., Calçada, R.: Calibration of the numerical model of a stone masonry railway bridge based on experimentally identified modal parameters. Eng. Struct. **123**, 354–371 (2016)
25. Aydin, A.C., Özkaya, S.G.: The finite element analysis of collapse loads of single-spanned historic masonry arch bridges (Ordu, Sarpdere Bridge). Eng. Fail. Anal. **84**, 131–138 (2018)
26. Weber, W.K.: Die gewölbte Eisenbahnbrücke mit einer Öffnung. Begriffserhlärungen, analytische Fassung der Umrisslinien und ein erweitertes Hybridverfahren zur Berechnung der oberen Schranke ihrer Grenstragfähigkeit, validiert durch einen Grossversuch. Dissertation, Lehrstuhl für Massivbau der Technischen Universität München (1999)
27. Barenblatt, G.I.: Dimensional Analysis. Gordon and Breach Publishers, London (1987)
28. Brencich, A., Corradi, C., Gambarotta, L.: Eccentrically loaded brickwork: theoretical and experimental results. Eng. Str. **30**, 3629–3643 (2008)

29. Royles, R., Hendry, A.W.: Model tests on masonry arches. Proc. Inst. Civ. Engrs. **91**, 299–321 (1991)
30. Brencich, A., Pera, D.: A new retrofitting technique for masonry arch bridges In: Bien, J. (ed.) 8th International Conference on Arch Bridges, ARCH 2016, Wroclaw, pp. 751–758 (2016)
31. UIC: UIC 778–3, 2nd Edition, Recommendations for the Inspection, Assessment and Maintenance of Masonry Arch Bridges (2011)
32. Brencich, A., Sabia, D.: Experimental identification of a multi-span masonry bridge: the Tanaro Bridge. Constr. Buil. Mater. **22**, 2087–2099 (2008)
33. RING 3.2 Users Manual: LimitState Ltd., Sheffiled, U.K. (2016)
34. Cavicchi, A., Gambarotta, L.: Two-dimensional finite element upper bound limit analysis of masonry bridges. Comput. Struct. **84**, 2316–2328 (2006)
35. Page, J.: Masonry Arch Bridges, State-of-the-Art-Review. T.R.L., D.o.T., HMSO, London (1993)
36. Darby, J.: Repair, strengthening and replacement. In: Ryall, M.J., Parke, G.A.R., Harding, J. E. (eds.) Manual of Bridge Engineering, Thomas Telford (2000)
37. Brencich, A., Colla, C.: The influence of construction technology on the mechanics of masonry railway bridges. In: Forde, M. (ed.) 5th International Conference and Exhibition Railway Engineering (2002)
38. Brencich, A., Pera, D.: A low-cost retrofitting technique for masonry arch bridges: experimental validation. In: Proceedings of the IABSE Symposium, Guimaraes, March 2019, pp. 37–45. IABSE, Zurich (2019)
39. Modena, C., Tecchio, G., Pellegrino, C., da Porto, F., Donà, M., Zampieri, P., Zanini, M.A.: Reinforced concrete and masonry arch bridges in seismic areas: typical deficiencies and retrofitting strategies. Struct. Infr. Eng. **11**(4), 415–442 (2015)

History of Arch Bridges in Portugal

Júlio Appleton[1,2(✉)]

[1] A2P Consult, Lda, Lisbon, Portugal
julio.appleton@a2p.pt
[2] Instituto Superior Técnico, Departamento de Engenharia Civil, Arquitectura e Georrecursos, Lisbon, Portugal

Abstract. This work presents some arch bridges constructed in Portugal since the Roman Empire period to recent times. For some masonry. Steel and concrete bridges construction details are also presented. Bridges and all constructions requires permanent maintenance. Some old bridges presents a reduced deck width requiring its enlargement. Live loads increased along time requiring strengthening interventions in existing bridges. The most severe action that led to some bridge destruction is river flooding and foundation infraescavation.

Some examples of interventions are presented in the paper.

Keywords: Bridges · History · Arch

1 Introduction

For centuries arch masonry bridges were the most used solutions to cross rivers and other obstacles. With this structural solution the stones are subjected to compression for which the material has a much higher strength than for tension.

The span of the vaults was, in general, less than 20 m and, so to cross large valleys, multiple arches were needed.

From 1840, with the industrial revolution, new steel bridges were constructed. The use of steel allowed much bigger spans and made much easier the transport and elevation of structural elements.

In 1875 Monier constructed the first concrete arch bridge that still followed the conceptual design for masonry bridges. Concrete arch bridges are being constructed to the present day.

The objective of this work is to present some of the arch bridges constructed in Portugal [2].

2 Masonry Bridges

During the period of the Roman Empire in Iberia several bridges were built in the road network established to connect Portugal to Rome [9].

The masonry arch bridges had a cylindrical vault geometry.

Two of the most well-known bridges in Portugal are those presented in Figs. 1 and 2.

A. Arêde and C. Costa (Eds.): ARCH 2019, SI 11, pp. 31–50, 2020.
https://doi.org/10.1007/978-3-030-29227-0_2

Fig. 1. Bridge over Ribeira de Seda in EN 369 between Ponte de Sôr and Alter do Chão [2]. a2p archive

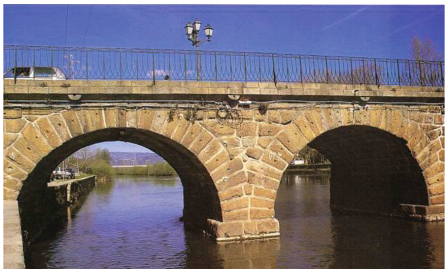

Fig. 2. Bridge over Ribeira de Seda in EN 369 between Ponte de Sôr and Alter do Chão [2]. a2p archive

The span of these bridges did not, in general, exceed 20 m and the thickness of the piers were of the order of 1/3 to 1/5 of the span.

To build these bridges they developed technics for cutting stone blocks and for its transportation and elevation, as shown in Figs. 3 and 4.

Fig. 3. Forfex used from antiquity to present time [2]. a2p archive. www.viasromanas.pt

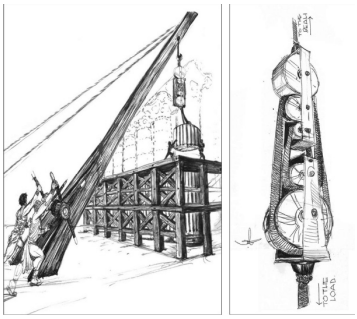

Fig. 4. tripastos and pentapostos for elevation of big weights [11]. Rababeh Shaher

Irregular stones and rubble were placed over the arches and between spandrel walls, as shown in Fig. 5.

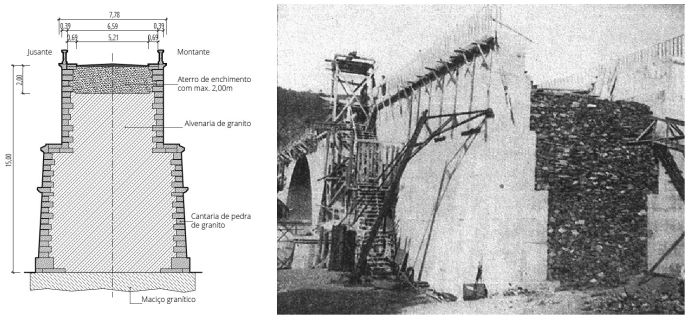

Fig. 5. Transverse section of a pier and abutment (left drawing ref. [3]), (photograph ref. [6]) JAE and IP. a2p archive

Arch bridges continued to be constructed for centuries. In 1744, just some years before the devastating earthquake that destroyed Lisbon, the Aqueduct of Alcântara (with 35 arches, part of the project of a 14,1 km water supply) was erected. The main arch has 28,86 m span and is 69,29 m high (Fig. 6). No significant damage occurred in that structure during the 1775 earthquake.

Fig. 6. Aqueduto das Águas Livres in Lisbon, [2] a2p archive

Two of the main problems of the old arch bridges are the reduced deck width for the present traffic needs and the reduced flood section capacity.

Figure 7 illustrates the River Ponsul bridge in EN 240 at km 12,2. Built in 1875, that bridge had its deck enlarged from 7,20 m to 11,50 m in 2007. The bridge has 3 arches of 13,40 m span.

Fig. 7. Deck widening with a new prestressed concrete slab over the masonry bridge, [2] a2p archive

Figure 8 shows Barão Bridge, located at EM 526 between Loulé and Albufeira, that has had the deck enlarged from 3,6 m to 8 m and the flood section increased by the introduction of a new arch and lowering the river bed, with simultaneously strengthening of the foundations.

Fig. 8. Deck widening with precast slabs longitudinal posttensioned [2] a2p archive

In Fig. 9 the railway Poço de S. Tiago Bridge designed by the French engineer Séjourné and constructed in 1913 by a French company (François Mercier) is presented, together with the graphics for the calculation of the bridge. The bridge has a total length of 168 m with a central arch of 55 m span and 24,70 m rise.

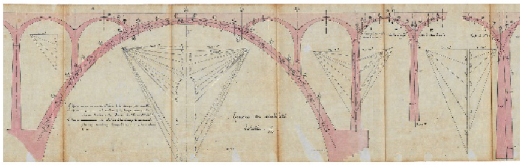

Fig. 9. Poço de S. Tiago bridge and calculation graphic JAE and IP. IP archive

Figure 10 illustrates a masonry arch bridge that has had a partial collapse due to the rotting of the wooden piles. This accident was the result of the lowering of the river bed due to sand exploration downstream of the bridge location. In this situation the wood piles were dried and exposed to the environment in the drought period.

Fig. 10. Partial collapse due to wooden pile rot [2] a2p archive

One of the last arch bridges constructed in Portugal was the Abragão Bridge in EN 320 with a 60 m span built in 1944 according to the design of Edgar Cardoso. Figure 11 illustrates this bridge (now submerged by a dam reservoir) and some of the tests done to check the bridge design.

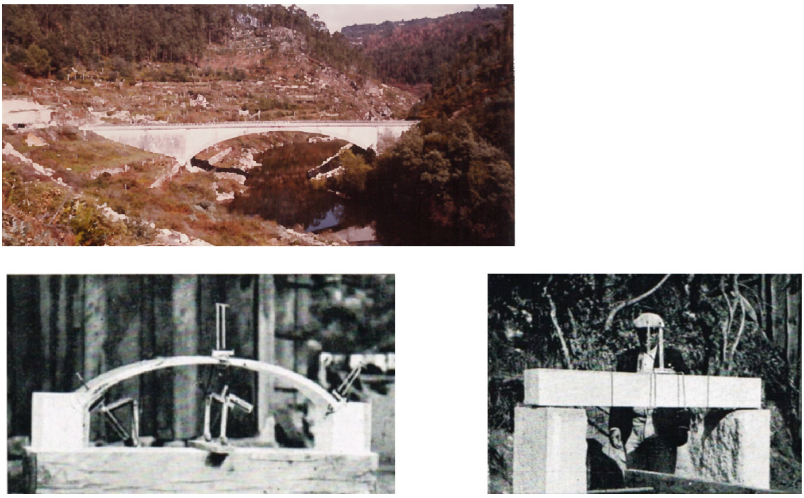

Fig. 11. Abragão Bridge in EN 320 and design models [5] JAE and IP. Edgar Cardoso

3 Steel Bridges

The most important steel bridge in Portugal is the Maria Pia Arch Railway Bridge over Douro River in Porto/Gaia. The bridge, built by the Eiffel Company according to the structure design of T. Seyrig (Fig. 12), was inaugurated in 4/11/1877 [8].

The bridge has a hinged arch with 160 m span and 42,60 m rise. The arch has the maximum thickness of 10 m at the crown. The width varies from 3,95 m at the crown up to 15 m at the springing line, for transverse stability of the bridge (Fig. 13).

The execution of the arch was done by successive cantilevers supported by stays fixed in the rock (right margin of Douro, Porto side) or at the abutment (Gaia side). The deck was assembled at the abutments and pushed to the final position over the steel columns (Fig. 14).

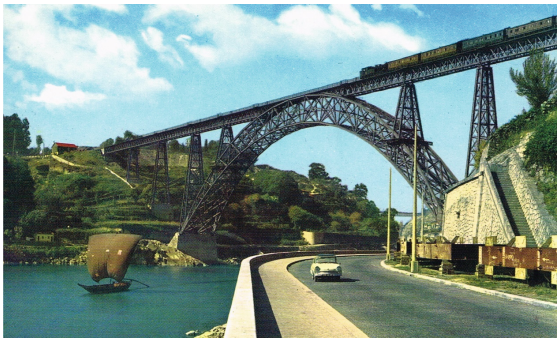

Fig. 12. Maria Pia Bridge over the Douro River Luxocolor Esmaltex

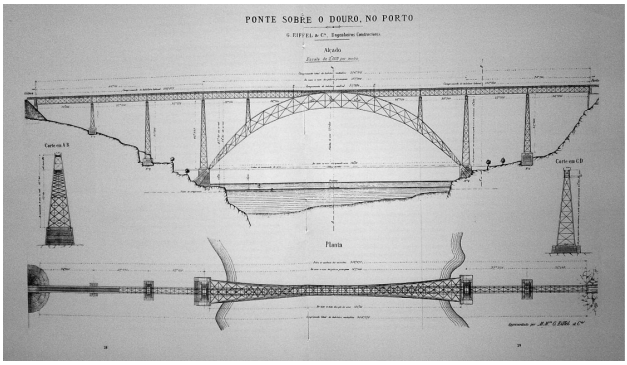

Fig. 13. Plan and elevation of Maria Pia Bridge [12] Eiffel

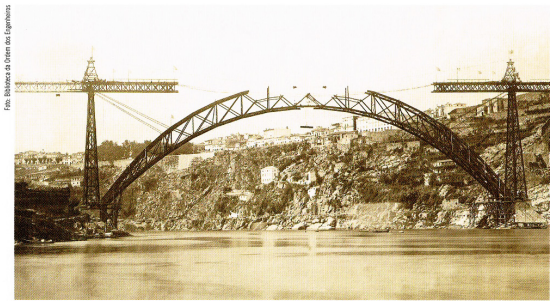

Fig. 14. Construction stage of Maria Pia bridge in 15/8/1877 [10] Vasconcelos

The bridge was replaced in 2000 by the São João Bridge and, up to now, has not been in use, which is negative for its future preservation.

Not far away from this bridge stands Luis I Bridge over Douro, a bridge with 2 decks, one at the top of the arch and another at the level of the springing line (Fig. 15). This bridge was constructed by the Willebroek Company according to a design of T. Seyrig, to replace the Porto Pensil bridge. The arch has a 172 m span and 45,10 m rise. Recently the top deck was adapted to install a Porto Underground line.

Fig. 15. Luiz I Bridge over Douro river in Porto Not identified author of postcard

In 1919 a bowstring bridge was built for the Algarve railway line in Portimão over the Arade River. The bridge was constructed by "Empresa Industrial Portuguesa" and has 6 spans of 50 m (Fig. 16).

Fig. 16. The Portimão railway bridge over the Arade River, [2] a2p archive

In 1951 another bowstring bridge was built over Tagus Bridge at Vila Franca de Xira for the Road Authority (JAE). It includes 4 × 103,50 m spans. This bridge was constructed by the consortium Dorman Long & Loyd and the Portuguese Company Seth. Each span was assembled over a simple supported truss, as shown in Fig. 17.

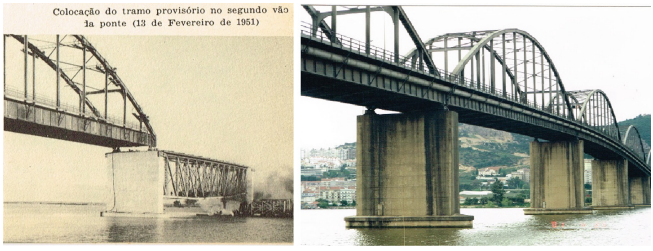

Fig. 17. The Vila Franca de Xira Bridge and the provisional truss for the arch assembly [2] a2p archive. JAE and IP [13]

The first concrete pile tests in the Tagus River were performed for this bridge (Fig. 18). The driven piles with 50 cm diameter and 32 m long were made of precast reinforced concrete.

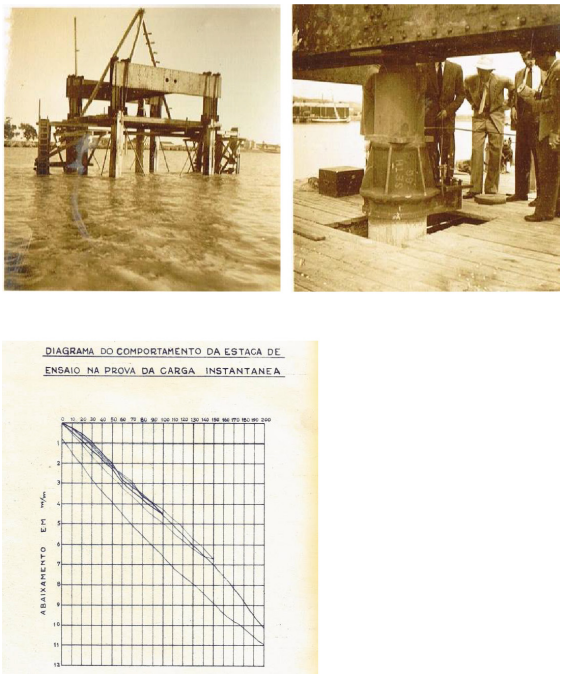

Fig. 18. Pile tests at the site of the Vila Franca de Xira Bridge [14] Lopes Alves

In these constructions, the steel structure elements were made of steel plates and L sections assembled by rivets, as shown in Figs. 19 and 20.

The bearings were made with cast iron or steel, as shown in Fig. 21.

The execution of the first steel bridges in the 19th century and first half of the 20th century is associated with the period of the industrial revolution and the need to create a railway network and ameliorate the road network [7].

In the same period, an enormous progress occurs in the structure mechanics modelling, in the structure scaled models and in situ evaluation of structure behaviour. Further significant developments in structural mechanics only occurred later, in the 60s of the 20th century, with the new computing facilities and structure numerical modelling.

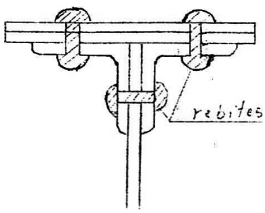

Fig. 19. Typical assembly of steel elements by rivets Edgar Cardoso

Fig. 20. Application of rivets in rehabilitation works a2p archive

Fig. 21. Steel Fixed and sliding bearings a2p archive

The main anomalies in steel bridges are the deterioration of the surface protection, the cracking due to fatigue and buckling of excessive compressed elements. Many old bridges required strengthening interventions due to the increase of live loads or due to insufficient deck width or the need to increase the vertical clearance.

The interventions in steel structures may be done with strengthening or replacement of elements or the application of external prestressing.

4 Concrete Bridges

The first concrete bridges constructed in Portugal in the beginning of the 20th century were arch bridges. One of these was the Luis Bandeira Bridge near Sejães (Oliveira de Frades) on the Vouga River in the EN 333-3, recently submerged by a dam's reservoir (Fig. 22).

It was constructed by Moreira de Sá e Malevez in 1907, according to the construction procedures and patents of Hennebique Company. It has an arch of 44 m span.

Fig. 22. The Luiz Bandeira Bridge in EN 333-3 over the Vouga River near Sejães, [1] a2p archive

Many arch bridges were constructed in the XX century, such as the Chaminé Bridge over the Ribeira de Mora in EN2 km 474 between Montargil and Mora (Fig. 23) built in 1934. This bridge with three arches of 27,20 m and 3,40 m rise has had its deck enlarged from 6,75 m to 10,50 m in 1995 [6].

Fig. 23. The Chaminé Bridge a2p archive

In Lisbon, for the new west road along the coast, the Duarte Pacheco Viaduct on the Alcântara Valley was constructed in 1944 (Fig. 24). The viaduct (designed by Barbosa Carmona from the JAE Bridge Department), with a total length of 355,10 m, includes a central arch of 91,80 m. This arch was erected with a wood falsework supported on the ground (Fig. 24).

Fig. 24. The Duarte Pacheco Viaduct and some of its steel bearings. [2] a2p archive

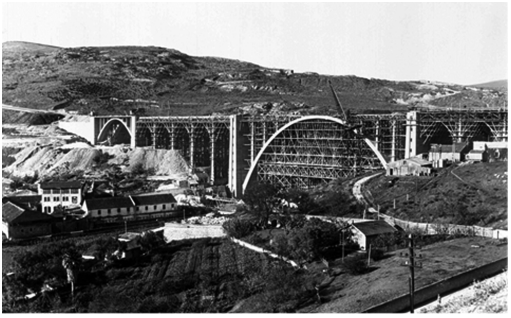

Fig. 25. Construction of Duarte Pacheco Viaduct JAE and IP

In 1952, a reinforced concrete bowstring bridge was built over the Sado River with a design of Edgar Cardoso, with two arches of 31,50 m span and a lower deck (Fig. 26).

Only in 1959 the first reinforced concrete arch bridge exceeding 100 m was constructed in Portugal. It was the Sousa Bridge with a main span of 115 m over the mouth of the Sousa River. In Fig. 27 a general view of this bridge is presented together with the wood falsework used for its construction.

Several multi-arch, bi-articulated bridges were constructed such as the Barca de Alva Bridge over Douro River designed by Edgar Cardoso in 1955 with 6 spans of 37,50 m (Fig. 28) and in 1959 the bridge over Trancão at A1 in Sacavém with 5 spans of 57 m, designed by Franco e Abreu and Rui Correia (Fig. 29). To note that in this bridge the posts supporting the deck and connected to the arch are not vertical.

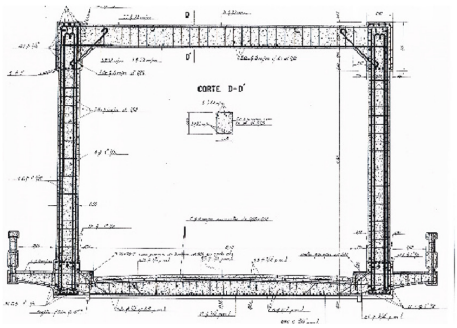

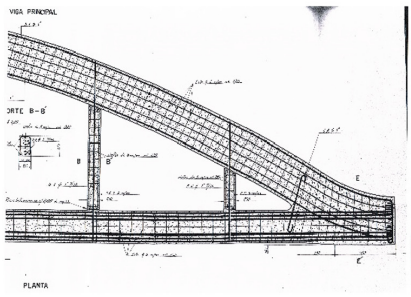

Fig. 26. Arch bridge and reinforced concrete structure details (photograph a2p archive, Drawings [15] a2p archive. Edgar Cardoso

Fig. 27. The Sousa Bridge (photograph a2p archive, also in ref. [2] and falsework for the arch Novopca archive) a2p archive. JAE and IP

Fig. 28. The Barca de Alva Bridge over the Douro River [10] Novopca

Fig. 29. The Trancão viaduct in A1, near Sacavém, a2p. [2] a2p archive

For the Trancão Viaduct the falsework was a steel structure (Fig. 30) used several times to construct each of the 6 parallel arches in each span.

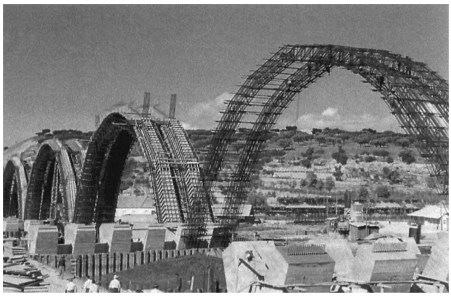

Fig. 30. Steel falsework for concreting the various arches [16] OE

Figure 31 shows the longitudinal geotechnical profile and the results of the pile tests carried on by LNEC (1 m diameter cast in situ reinforced concrete piles, 55 m long). At that occasion horizontal load test were also performed.

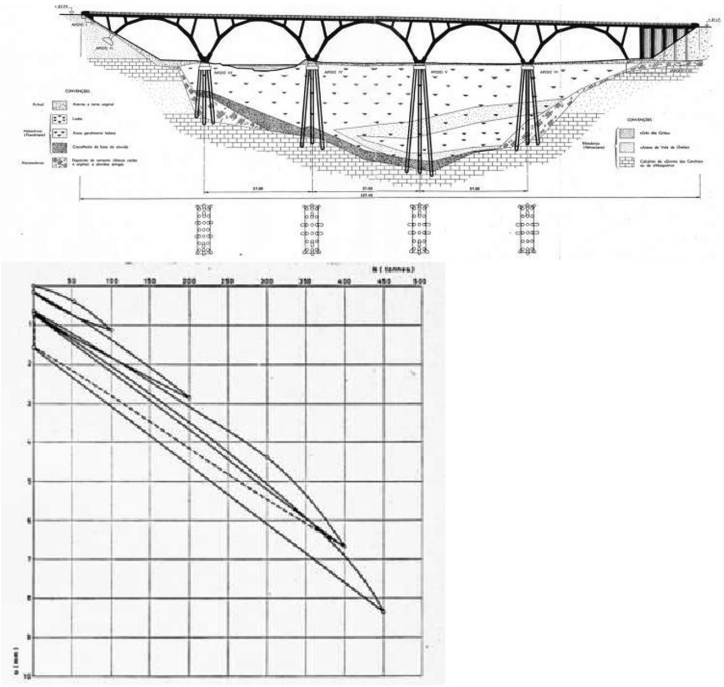

Fig. 31. Geotechnical profile and pile vertical load test results [17] LNEC

During the same period a flat arch bridge was built in 1957 over the Tua River with a span of 92 m and rise of 9,20 m (Fig. 32). This bridge was designed by Correia de Araujo and Campos e Matos.

Fig. 32. The Abreiro Bridge and its designers during a site visit António Fonseca (FEUP). Matos Fernandes (FEUP)

The reference arch bridge in Portugal is still the Arrábida Bridge built in 1963 over the Douro River between Porto and Gaia with 270 m span [4], a world record at the time (Fig. 33).

The 493,20 m continuous deck and highly hyperstatic structure required extensive analytical and scaled model testing (Fig. 34), at the time the only possible methodology to access the global structure response. The bridge was constructed by Pereira Zagalo, according to the design of Edgar Cardoso.

Fig. 33. The Arrábida Bridge over the Douro River (a2p archive, also in ref. [4])

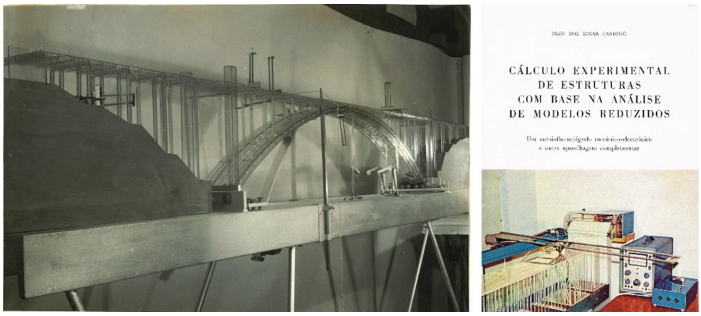

Fig. 34. Structure elastic model [18] Edgar Cardoso

A steel falsework was erected to construct one of the twin arches and afterwords transversely moved to execute the other arch and moved again to construct the connecting truss between the arches (Fig. 35).

Fig. 35. Completion of the falsework for the execution of the first of the twin arches [19] JAE and IP

To avoid the cost of the falsework, the most recent arch bridges were executed using the successive cantilever method with special temporary ties as used in the Zêzere Bridge in 1993 with a span of 224 m (Fig. 36) and the Infante Bridge, a stiffened deck arch, over the Douro River built in 2003 with 280 m span and a rise of 25 m (Fig. 37).

Fig. 36. The Zêzere Bridge in EN348 Vitor Barata

Fig. 37. The Infante Bridge over the Douro River António Fonseca (FEUP)

This bridge has a slender arch and a strong deck. The thickness of the arch is 1,50 m and the width varies from 10 m to 20 m at the springing line. At the crown, the arch and the deck are join together and have a thickness of 6 m.

In Fig. 38 the relation, for a parabolic hinged arch, between the span/rise with the horizontal thrust for a uniformly distributed load is shown (H/V = 4f/l), to stress the importance of the arch geometry in the support reaction. Some arch bridges are hinged in the supports during the construction stage.

Nº	Name	Span l (m)	Rise f (m)	Span/Rise l/f
1	Trancão	51,6	18,6	2,77
2	Arrábida	270	52	5,16
3	Foz do Sousa	115	14,75	7,80
4	Abreiro	92	9,2	10.0

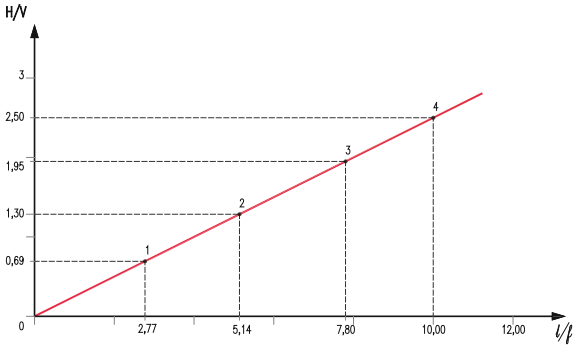

Fig. 38. Relation of arch thrust and its geometry [2] a2p archive

The main anomalies in reinforced concrete structures are the reinforcement corrosion and the chemical expansive reactions in concrete (ASR and ISR).

Structure strengthening can be done with section jacketing and additional reinforcement. To strengthen the deck an effective technique is the external prestressing.

5 Final Considerations

Arch bridges are robust and beautiful constructions that gave also value to the landscape.

Masonry arch bridges were constructed up to the middle of the XX century.

Steel bridges were very common in the end of the XIX century and beginning of the XX century. The cost of execution in Portugal reduced its application, revitalised in recent decades with mixed steel/concrete structure solutions.

Steel arch bridges over Douro continue to be some of the most beautiful bridges in our country.

Concrete arch bridges were constructed during the XX century using a wood or steel falsework. The development in prestressing and cable technology enabled the recent construction of arch bridges by successive cantileevers and back stays.

Arrábida bridge and Infant bridges over Douro in Porto/Gaia are two important landmarks and engineering achievements.

Figure 39 and adjacent table presents the relation between the arch span and the date of construction for some of the masonry, steel and concrete arch bridges constructed in Portugal.

Type	Name	Date	Span (m)
Masonry	Aqueduto Águas Livres	1748	28.9
	Ponte do Bico	1866	14.5
	Ponte Rio Ponsul	1875	13.4
	Ponte de Abragão	1944	60.0
Steel	Ponte Maria Pia	1877	160.0
	Ponte Luiz I	1886	172.0
	Ponte Ferroviária Portimão	1919	50.0
	Ponte Marechal Carmona	1951	103.6
Concrete	Ponte Luiz Bandeira	1908	32.0
	Ponte Roxo	1931	45.0
	Ponte Chaminé	1933	27.2
	Ponte Foz do Dão	1935	60.0
	Ponte Tua	1939	80.0
	Viaduto Duarte Pacheco	1944	91.8
	Ponte Arcos	1952	31.5
	Ponte Foz do Sousa	1954	115.0
	Ponte Barca de Alva	1955	37.5
	Ponte Abreiro	1957	92.0
	Viaduto Trancão	1959	51.6
	Ponte Arrábida	1963	270.0
	Ponte Zêzere	1993	224.0
	Ponte Infante	2003	280.0

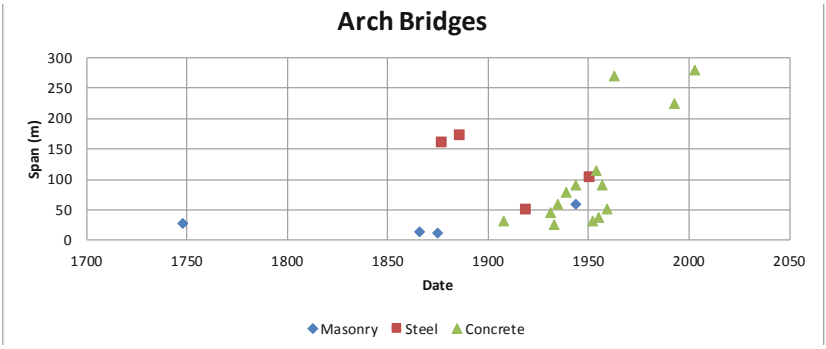

Fig. 39. Relation between date of construction and span for some arch bridges built in Portugal a2p archive

References

1. Appleton, J.: Betão Armado – Nota Histórica, Construção Magazine, nr 44 (2011)
2. Appleton, J.: Pontes em arco, ASCP (2005)
3. Appleton, J.: História da construção de pontes em Portugal, BE 2016 (2016)
4. Appleton, J.: Arrábida bridge, Arch (2001)
5. Cardoso, E.: Alguns Métodos de Cálculo Experimental e sua Aplicação ao Estudo de Pontes, Dissertação IST (1950)
6. Franco e Abreu, A.: Evolução da Construção da Ponte na Obra da JAE, MOP (1953)
7. Martins, M.R., Torres, M.T., Faria, P.: Pontes Metálicas Rodoviárias, JAE (1998)
8. OE: Região Norte – Ponte Maria Pia, OE (2005)
9. Soares Ribeiro: Pontes Antigas Classificadas, JAE (1998)
10. Vasconcelos, A.: Pontes dos Rios Douro e Tejo, OE (2008)

11. Rababeh, S.: Technical utilization of lifting devices for construction purposes in ancient Gerasa. Int. J. Archit. Heritage, 12/2014 (2104)
12. Eiffel, G.: Cie: Memória para apoio do projecto da Ponte sobre o Rio Douro próximo do Porto, Revista de Obras Públicas e Minas (1876)
13. JAE: Ponte Marechal Carmona, DSP (1951)
14. Alves, N.L.: Ponte sobre o Rio Tejo em Vila Franca de Xira, notas sobre o acompanhamento da obra de fundações (1952)
15. Cardoso, E.: Projecto da Ponte dos Arcos (1952)
16. OE: 100 obras de engenharia civil no século XX em Portugal (2000)
17. Folque, J., Castro, G.: Essai de chargement horizontal de pieux très longs, Memória 193 LNEC (1962)
18. Cardoso, E.: Projecto da Ponte da Arrábida sobre o rio Douro (1963)
19. JAE: Ponte da Arrábida (1963)

Arch Bridges or Bridges with Arches, Elegant and Efficient Solutions to Cross an Obstacle

Vincent de Ville de Goyet(✉)

Engineering Greisch, ULiege, Liege, Belgium
vdeville@greisch.com

Abstract. For 2000 years, the basic material to build a bridge was wood or stone. The typical shape of stone bridges was the semi-circular arch. The first bridges made of metal were again arch bridges where the internal forces are essentially compression forces. The industrial revolution and the progress of the theoretical knowledge in the field of structural mechanics made it possible to design bridges with different shapes. Bridges with large spans were mainly suspended and also arch bridges. Today, the arched bridges are probably very well suited for crossing very deep valleys or rivers in an area without relief.

Keywords: Arch bridges · Tied arch bridges · Design · Construction methods

1 Arches in the Nature

We can say that the first arches were built by nature, by the erosion. Some are quite impressive as the Owachomo bridge or the Rainbow bridge (Fig. 1).

Fig. 1. Owachomo bridge and Rainbow bridge (US)

Until the 19th century, the basic material for building a bridge was stone and its shape was the arch. The best known is the Pont du Gard (F), an ancient Roman aqueduct bridge built in the first century AD. The Limyra footbridge (TR) is another example of masonry bridge, built in the third century AD (Fig. 2). The stone or masonry was the best material for this type of structure because their internal forces are compression forces. The development of steel during the industrial revolution and the progress of the theoretical knowledge in the field of structural mechanics made it

A. Arêde and C. Costa (Eds.): ARCH 2019, SI 11, pp. 51–70, 2020.
https://doi.org/10.1007/978-3-030-29227-0_3

possible to design bridges with different shapes, mainly suspension bridges and also arch bridges.

Fig. 2. The Pont du Gard - 48 m (F) and the Limyra footbridge - 15 m (TR).

2 Evolution of the Building Material and of the Bridge Shape

The Coalbrookdale bridge, also called Iron Bridge, on the Severn River (UK, 1779) (Fig. 3) is the first metal bridge in the world. It is still used today for pedestrians. The structural behaviour of cast iron multiple arches bridges is similar to arch bridges in stone masonry. It develops only compression stresses. With the discovery of the iron, it was possible to imagine structures in which there are tension forces. With this material, bridges with larger spans appeared, essentially suspension bridges as the Menai bridge, designed by Thomas Telford and completed in 1826.

Fig. 3. Iron bridge - 60 m (UK) – The Menai bridge - 176 m (UK).

But it enables also the development of large arches, by means of trusses composing the arches, as for the two major viaducts of Gustave Eiffel, the bridge Maria Pia in Porto (1877) and the viaduct of Garabit (1884) (Fig. 4).

Fig. 4. The Garabit bridge - 165 m (FR) – The Maria Pia bridge - 160 m (PT).

With its mechanical characteristics far superior, steel gradually replaces iron in all types of structures and allows more slender structures. Resistant to both traction and compression, steel gives the possibility to imagine lattices whose overall stability is ensured by only normal efforts. The advantage of this lattice-based design was to build a large structure with elements of limited size, easy to transport and to assemble on site (Fig. 5).

Fig. 5. Harbour bridge - 503 m (1932-AU) – Bayonne bridge - 510 m (1931-US).

3 Bridges with Arches

3.1 Typologies

From that time on, the arch bridges were declined in different forms by arranging the deck either above the arch (a), under the arch (b) or at mid-height (c). In the configuration (b), it is called tied-arch Bridge (Fig. 6).

The choice of one or the other configuration depends essentially on the obstacle to be crossed:

- the arch below the deck (a): very hilly region
- the arch above the deck (b): area without relief
- the deck at mid-height (c): intermediate situation

and the mechanical characteristics of the soil:

- for configurations (a) and (c), the critical aspect is the foundations of the arch which require a soil with good mechanical properties to be able to take over important compression inclined forces
- the tied-arch bridge is self-stable: the compression of the bow is taken up by the deck and the only reactions are only vertical.

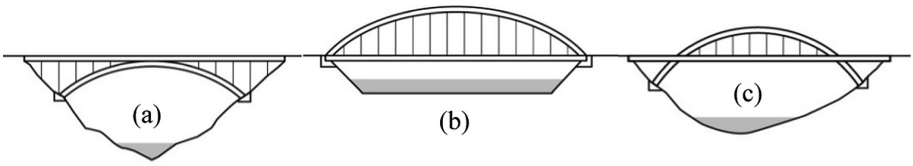

Fig. 6. Different configurations of bridges with arches

The span length/arch height ratio of the arch is often in the range of 5–6 for economic reasons. The deck is positioned at the level of the abutments. Its thickness is relatively limited because it is supported by the hangers (config b and c) or by the columns (config a) that can be considered as multiple supports whose inter-distance is small. It is therefore solicited by bending moments between these supports. In the case of tied arch bridge, the deck will also be in tension.

3.2 Deck Above or at Mi-Height of the Arch

In the two configurations (a) and (c), even if the arches are in compression, the risk of instability is reduced because of their connection with the deck. The arches can be either restrained or articulated at the base.

3.3 Arch Above the Deck

In this case, we speak of tied-arch or bow-string bridge by analogy of form with a bow with its stretched rope. The arches are not held by the deck. They are generally connected in their upper part by a so-called bracing structure, often composed of transverse beams. They ensure their transverse equilibrium, for example under the action of the wind and to avoid the risk of instability.

3.4 The Size of Arch Bridges

The length of the main span is the most common way to rank bridges as it usually correlates with the engineering complexity involved in designing and building the bridge. Whatever the configuration, the main difficulty for this type of bridges is its construction. Often,

- for tied arch bridge, the structure is often assembled with temporary piers on the waterfront and transported to its final location with flat boats,

Fig. 7. Construction methods for arch bridges

– for other arch bridges, the arch is often constructed using the cantilever method (Fig. 7)

The difficulty of its construction is one of the reasons of the maximum span length of arch bridges effectively built and of its ranking among the different types of bridges (Fig. 8), beam bridge, arch bridges, cable-stayed bridges or suspension bridges. The Fig. 9 shows the main span length of the arch bridges and the year of the construction. Only bridges with span length greater than 200 m are mentioned. It is clear that

– the evolution of the lengthis due to the method and not to the evolution of the construction material
– today, the maximum length is 552 m for steel arches (Chaotianmen Bridge - CN), 445 m, for concrete arches (Qinglong Railway Bridge - CN) and 530 m for steel arches with concrete inside (Bosideng bridge - CN) (Figs. 9 and 10).

Harbour Bridge (Fig. 5), in Sydney, with its 503 m, is well-known. It was the world record during 45 years. The arch is composed of two 28-panel arch trusses. Todays, the section of many arches are composed of steel or concrete beams as, for example, as the Lupu Bridge (503 m) or the Quinglong railway bridge (445 m) (Fig. 10).

Fig. 8. Maximum main span length of bridges

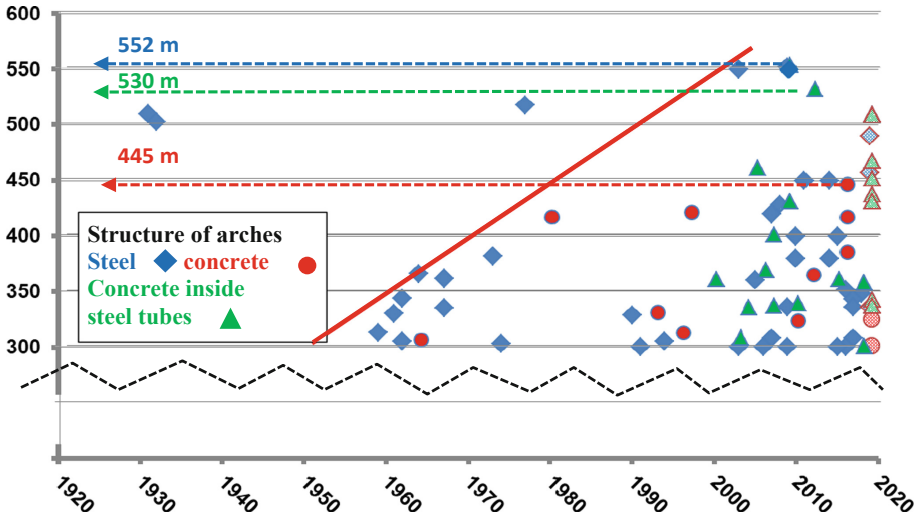

Fig. 9. Main span of arch bridges versus the arches structure and the year of construction

Fig. 10. Chaotianmen (steel-552 m) and Qinglong railway bridge (concrete-445 m)

4 Tied Arch Bridges

4.1 Interest of Tied Arch Bridges

The tied arch bridges are particularly well suited for crossing a pass in a flat landscape. The deck is stretched over its entire length and bended between its hangers (Fig. 11). It therefore has a low height; the access ramps have a shorter length than for a beam bridge with a higher deck height (Fig. 12). The deck is suspended at one or two arches arranged in vertical or inclined planes. Bowstring bridges are internally, statically indeterminate systems and externally, determinate systems. They are supported on simple bearings.

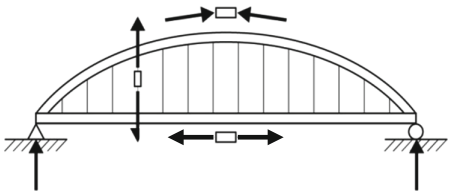

Fig. 11. Internal forces

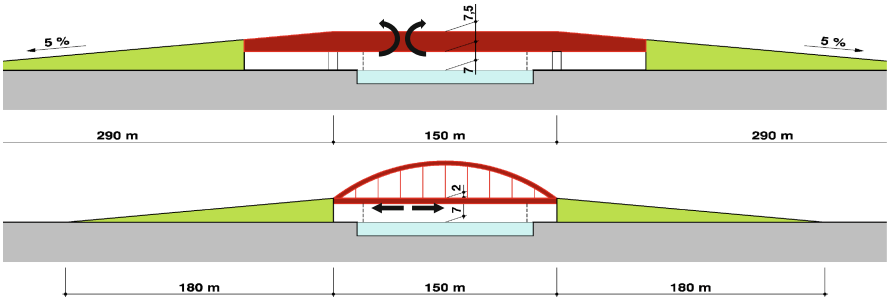

Fig. 12. Approach spans combined with two types of bridges

4.2 Tied Arch Bridges on the Albert Canal

The Albert Canal, which connects the river port of Liege with the seaport of Antwerp (Belgium), has been widened to allow traffic of push convoys of four barges with a whole capacity of 9000 tons. This decision has required the replacement of the existing bridges by new structures with a much longer span (roughly 150 m instead of 95 m). In the vicinity of Liège (B), the choice was stay cables bridges (Lixhe, Lanaye and Wandre) and tied arches bridges (Haccourt, Hermalle, Marexhe and Milsaucy – Fig. 13).

In northern Belgium, a flat country, there are numerous examples of tied arches bridges. They are entirely concrete bridges. The arches are braced over great length and the hangers are vertical. The set of deck, arch and hangers works like a Vierendeel beam. For the new bridges, the objectives were to obtain slender structures, easier to build also with no (minimum) interruption of the boats river traffic. Designed in the same period, they gave an opportunity to try to optimize each structure, to adapt each one to the local configuration and to take advantage of the latest theoretical developments in the field of instability. Even their main span length was almost the same, each bridge is different (Table 1).

The hangers are locked-coil cables. Crossed cables (Fig. 14) have been preferred to vertical and parallel ones for two reasons: to ensure a better distribution of the traffic loads to the arches (Fig. 13) and to obtain a truss behaviour of the set of deck, arches and hangers. But, with this arrangement, it must be admitted that it also has some disadvantages: all cables are not in the same plane and, when the arches are inclined, as for the Hermalle bridge, the view of the suspension system is not clear (Fig. 13).

Table 1. Main characteristics of the bowstring bridges on the Albert Canal

Location	Main span L (m)	L/f (-)	Width (m)	Arches	Bracing shape	Bracing location, $\alpha = X/L$
Haccourt (B)	139.5	6	20.90	2, parallel	/	/
Hermalle (B)	138.1	6	15.60	2, inclined	1 transversal top beam	0.5
Marexhe (B)	100.18	5	18.30	2, parallel	2 transversal beams	0.25/0.75
Misaucy (B)	145.0	6	15.50	2 parallel	2 St. Andrew's crosses	0.20/0.80

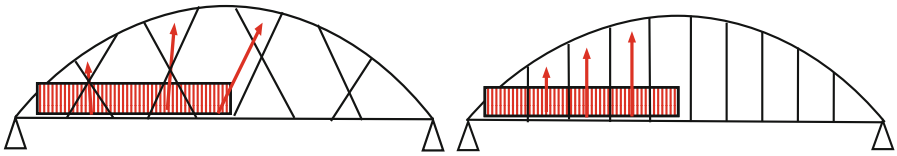

Fig. 13. Inclined/vertical hangers and traffic loads

Fig. 14. Tied arches bridges on the Albert Canal.

4.3 Behaviour of the Arches

The arches are in compression. Their stability must be verified. Often, the instability in the arches plane is not preponderant; the first buckling mode appears transversally. For this mode, the arch can be considered as a beam, with compression stresses, restrained to the deck at each end. But in contrast with a simple compressed beam for which the ratio of the first two critical loads is 4.0, in the case of tied arch bridges, this ratio is around 1.0. The origin of this result is the stabilizing effect of the stretched hangers. The transversal instability of the arches is equivalent to a compressed beam on elastic

foundation. Based on several scientific papers and researches at the University of Liège, the stabilizing effect of the tension hangers has been considered to better understand this behaviour and also to optimize the rigidity and the location of the transversal bracing between arches [1–4].

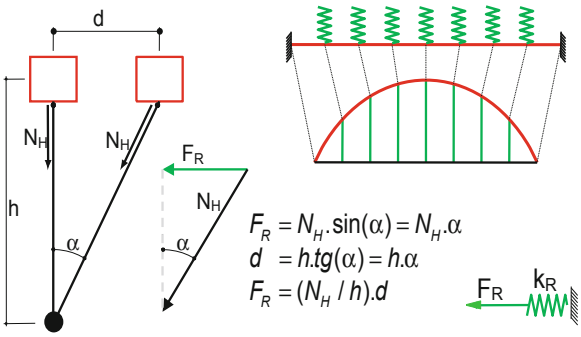

Fig. 15. Elastic foundation induced by hangers

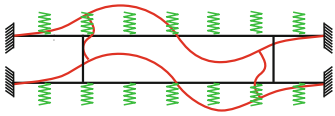

Fig. 16. Model to analyze the arches buckling.

For a pre-design, it can be considered that the buckling length of the compression arch is equal to 0.35 L*, with L*, the developed arch length. The first instability mode shape is the same one as for the second buckling mode of a compression beam full restrained at each support (Figs. 15 and 16). Based on a parametric analysis of the arch bracing, a simple design method, [1–4], has been suggested which allows a satisfactory accurate assessment of the critical out-of-plane buckling load of arches. This method simply consists of evaluating analytically the instability of the set of bracing and arches submitted to compression in the transversal plane of the arches supported by an elastic foundation for which the rigidity is equivalent to N_H/h (Fig. 15). Based on a parametric analysis of the arch bracing, a simple design method, [4], has been suggested which allows a satisfactory accurate assessment of the critical out-of-plane buckling load of arches. This method simply consists of evaluating analytically the instability of the set of bracing and arches submitted to compression in the arches transversally supported by an elastic foundation. This simple approach compared to the numerical values obtained by a finite element software shows that the understanding of the instability phenomenon is correct. The Fig. 17 shows the value the first critical transversal mode of the arches versus the location of the transversal bracing. The assumptions are: elastic constitutive law (Euler assumption) bracing beams with hollow cross section, only two bracing beams arranged symmetrically. It can be seen that the effect of the bracing beams is optimum with a location of 0.21 L* or 0.41 L*, with L*, the developed length of arches. With tacking into account the plasticity and the second order effects, the gain is lower but the optimal location of the bracing is the same (Fig. 18).

The efficiency of the bracing is clear but it is also possible to ensure the stability without it. For the four bridges on the Albert Canal (Fig. 13), four solutions to ensure the transversal stability has been used:

– Hermalle bridge: inclined arched ‘connected’ at the arches top
– Marexhe bridge: two transversal beams
– Milsaucy bridge: two St. Andrew’s cross beams
– Haccourt bridge: without bracing.

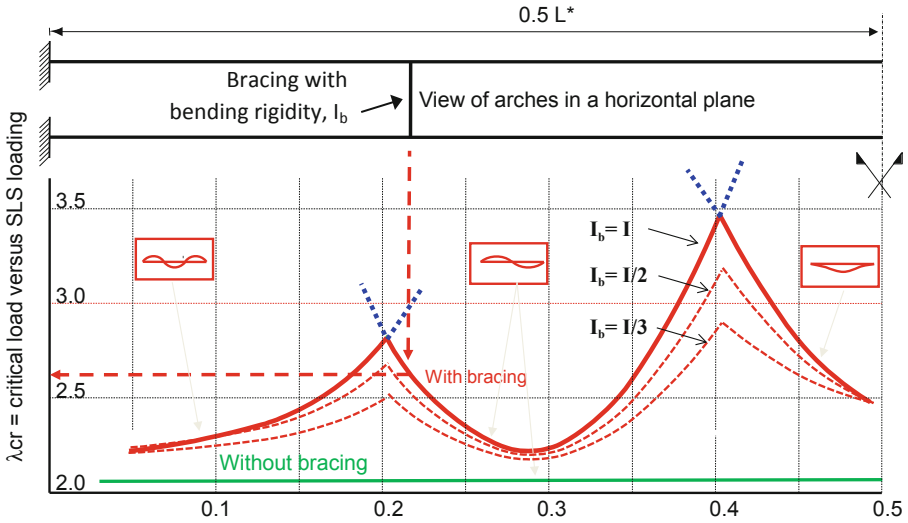

Fig. 17. Buckling load versus the location of bracing (x/L*).

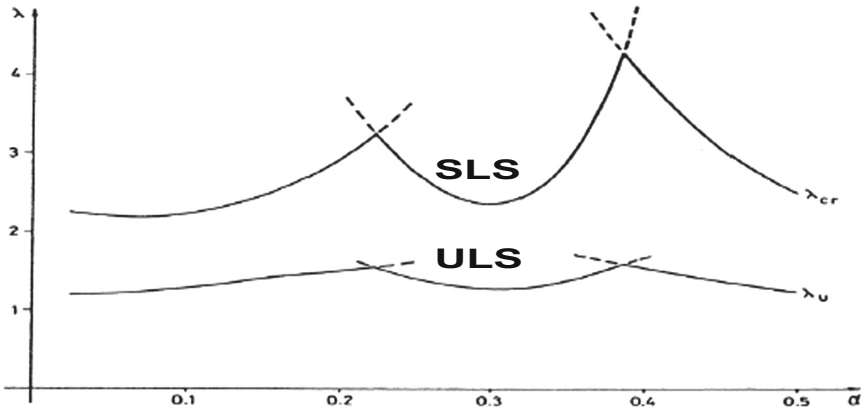

Fig. 18. SLS, ULS instability load respect the location of the bracing

The deck of the Haccourt bridge is larger. A bracing with transversal beams was also possible but the dimensions of the beam cross section would be also greater to obtain sufficient rigidity not only to ensure the stability but also to support its own dead load. The solution was to suppress the bracing and to increase the bending rigidity of each arch. It is clear that, in that case, the hollow cross section of the arches must be larger to obtain the required stability.

For the Hermalle bridge (Fig. 17), with inclined arches, during their transversal displacements, each arch leans against the other; this behaviour adds a rigidity effect to the stabilizing effects of the stretched hangers. To incline arches seemed to be an elegant solution; the stability is increased. After several years of its opening, despite a comfortable road clearance, the trucks move laterally to the left of the traffic lanes when entering the bridge. Apparently, the trucks drivers are afraid to touch the arches. Perhaps, it would be interesting to increase the distance between the arch bases but, in this case, the deck width would also be increased.

The main stresses in the arches are in compression and the plate buckling must be verified. Thirty years ago, it was classical to ensure the plate stability by numerous stiffeners. Moreover, the loss of efficiency under compression stresses is classical for the webs. For the upper and bottom flanges, a supplementary loss of efficiency appears due to the curvature of the plates (Fig. 19). Under compression stresses, S1 and S2, in the plates plan, forces, TS, appear transversally. In the projects designed by the Belgian administration, each plate was stiffened with a few T profiles along the whole length of the arches (Fig. 19).

Researchers have been made in the University of Liège to design this type of plates, [5, 6]. For the final design, it has been proposed to suppress each stiffener in order to limit the final cost. Of course the double loss of efficiency due to the plate buckling and to the transversal forces, TS, has been taken into account. It was more interesting to increase the plate thickness than to weld stiffeners and so to decrease the cost of construction. Nonlinear simulations have been made with a finite element program to verify these assumptions.

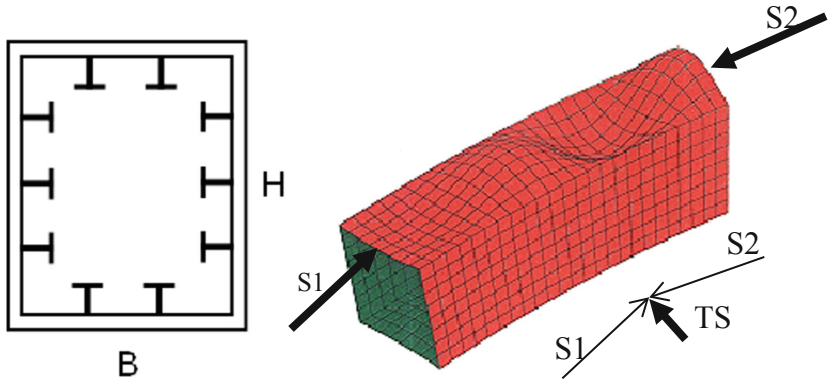

Fig. 19. Arch flanges in compression

4.4 Erection Methods

After the brittle collapse of some steel bridges in Belgium between 1938 and 1940, the welding of steel elements on the work site was prohibited until the mid-nineties. Therefore, the final connections of the arches for the new tied arches bridge on the Albert Canal have been made with bolts (Fig. 13).

Two of these tied arch bridges have been erected with temporary steel piers to assemble the deck and the arches: Milsaucy and Marexhe bridges. The two other, Hermalle (Fig. 20) and Haccourt bridges, have been assembled on the ground and after that, transported on flat boats to install them on their final position.

Fig. 20. Hermalle bridge on flat boats (1985)

4.5 Evolutions of the Design

Chanxhe and Chaudfontaine Tied Arch Bridges

After the design of the tied-arch bridges on the Albert Canal, some other bridges with the same typology have been imagined and designed. The stability of the compression was well-known and understood; we could focus on other details of the structure. Two tied-arch bridges, with a span length around 50 m, have been designed in Chanxhe and Chaudfontaine (Belgium) (Fig. 21).

Fig. 21. Chanxhe bridge and Chaudfontaine bridge.

The hangers are vertical and there is no bracing. With a ratio between the span length, L, and the arch top level, f, equal to L/6, the road clearance would be difficult to be respected with a transversal bracing. Moreover, its suppression gives the impression of lightness. A red colour has been adopted for the arches and the hangers for the Chanxhe bridge. For the Chaudfontaine bridge, the same red colour has been chosen for the arches and the deck and the white colour, for the hangers. This choice highlights the structural lines of the structure.

Hoge Brug in Maastricht

When it is possible to imagine tied-arch bridges with two arches without bracing, why not a tied-arch bridge with a single arch?

The Hoge Brug in Maastricht (Fig. 22) is a footbridge and crosses the river Maas in the centre of Maastricht (NL). It constitutes a link for pedestrians and cyclists between the new modern Ceramique district and the old city. With a 164 m long main span without supports in the river, the bridge is perfectly integrated in its both modern and natural environment, but its elegance and its slenderness are also attractive. This impression of slenderness is due to the little dimensions of the structural elements (deck, arch, suspension cables) compared to their length, and is accentuated by the curve of the deck section, a box girder shaped as a sector of a circle. It is constituted by 5 inner boxes and is maximum 1.2 m high.

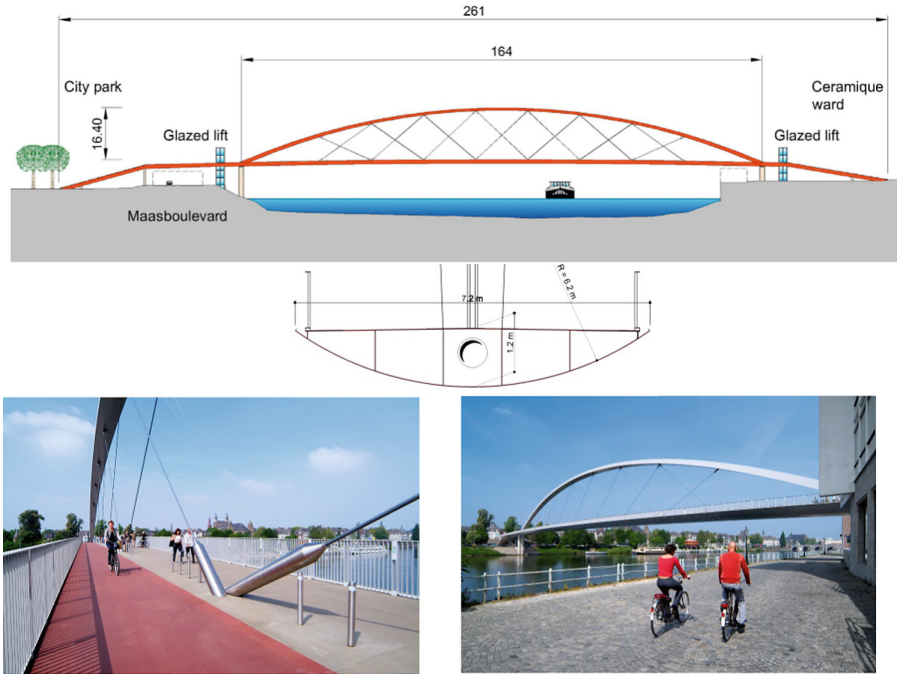

Fig. 22. Hoge Brig in Maastricht (NL)

The main span is suspended by 14 crossed cables fixed to a single central arch which its cross section has a variable geometry. So, at its basis, the cross section of the arch is 1.2 m wide by 1.2 m high, and at its top 2.4 m wide by 0.8 m high. By this way, the steel is distributed where it is efficient: a vertical rigidity at the basis to transmit the longitudinal moment to the deck and a transversal rigidity at the mid-span of the arch to ensure its stability. Its geometry reinforces yet the impression of slenderness. The single plane of hangers, anchored in the middle of the deck serves as a separation between the flow of pedestrians and cyclists. The main bridge was built on pontoons near its definitive position and was placed by barges driven by cables.

The Sado Viaduct

The railway Sado viaduct (Fig. 23) is located in the south of Portugal. To limit the number of piers in the river, the choice of a multiple tied-arch bridge has quickly been adopted: three successive tied-arch bridges with main spans length equal to 160 m. For the pre-design, two solutions were examined: tied arch bridges with two inclined arches or one vertical arch. Of course, for this comparison, the deck shape was different for the two solutions. With two longitudinal arches, the longitudinal rigidity is ensured by two longitudinal beams located, each one, below each railway track. A transversely eccentric vertical load is equilibrated by an alternated loading in each arch. For the case of single arch, the deck cross section must be a composite box girder, with a sufficient torsional rigidity to transmit the torsional moment to the bearings.

Both solutions were confronted with objective criteria on the basis of two preliminary designs carried out in parallel. Finally, the choice was made on the second design for different reasons. The single central arch is more effective. The critical load is greater and the overall deflection of the structure is lower. The variation of stresses in the hangers of the inclined arches is greater. This assessment is unfavourable for fatigue. The solution with two arches increases the number of elements to be assembled. The estimated cost for the two arches solution proved to be 10% higher. All these conclusions led to the final choice of three bowstring bridges with a single arch [7].

The steel hollow cross section of the arch has a hexagonal shape of which the height and the width are variable from the basis to the top. The width is increasing to ensure the transversal stability of the arch and the height is decreasing to have the maximum vertical bending rigidity at the connection with the deck. The ratio between the length of the span and the height of the arch is 5.40. The deck is suspended to the arch, every 8 m, by vertical and cylindrical solid bars. Their diameter is 200 mm with S355 steel quality. One particularity of the main bridge, composed of three tied arch bridges, is its continuity. Under the dead load, in spite of the continuity between the bridges, the bending moment between two bridges is quasi null. Under the variable load, it is not the case. This scheme doubtless distorts the behaviour of a real tied arch. But the interest was double: to suppress the problem of the rail track movement at the extremity of each tied arch bridge and also to have a single bearing device at the top of the concrete piers.

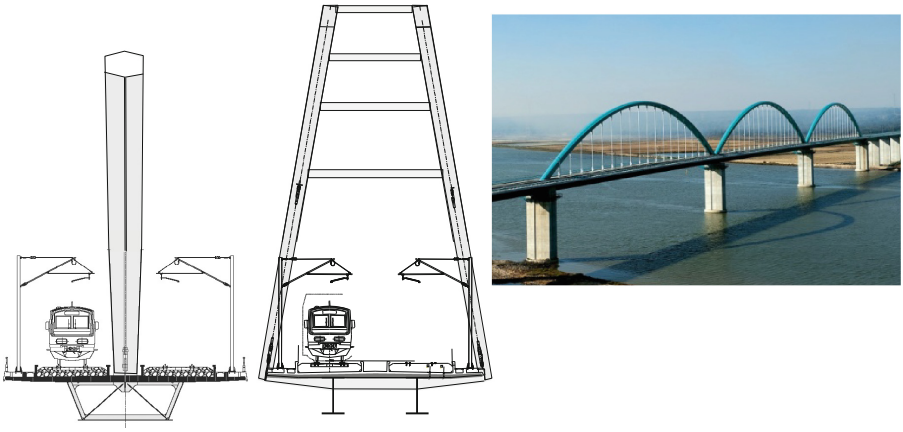

Fig. 23. Sado Viaduct (Portugal)

Assembled on temporary steel frames upwards of the river, the total length of the three spans of the deck has been built by launching. For that, two steel temporary piers have been installed in the river Sado between each final concrete pier. Temporary piers were also used to assemble the arches pre-fabricated in three elements. To adjust the internal bending moment in the deck due to the dead load after the launching, a vertical displacement of 1.3 m high has been imposed after the final launching. The instability of the arches has been verified with finite element simulations. The first critical eigen values being not so high by comparison with the ULS load level (2.55 and 2.75 ULS), nonlinear elasto-plastic computations have been realised with initial transversal deformed shape and several combinations of loading, dead load, wind and UIC loads.

5 Arch Bridges

5.1 Eau-Rouge Viaduct

The structure (Fig. 24) is located between Francorchamps and Malmedy on the E42 motorway (Belgium) close to the border with Germany. The aggressiveness of the valley bottom soil, required a central span of 270 m to avoid the area of ground with bad mechanical properties. This central span is crossed with two arches made of steel hollow rectangular cross sections with a distance of 14 m, supporting the composite deck via vertical members and diagonals. The approach spans are 258.75 m long north and 123.75 m south. The viaduct has a total length of 652.5 m. The composite steel-concrete deck is 27 m wide with two carriageways, each with two traffic lanes and one emergency stop lane. The two steel arches have a parabolic shape of minimum radius 150 m and a height of about 50 m. The two steel caissons are not interconnected by

any bracing except during the assembly phases. At the top of the arch, the arch and the deck are combined to form a single box of variable height (2.0 m up to 7.0 m) [8].

The special character of the structure, its lightness, its slenderness and the span length of the arch have led engineers to realize a series of numerical simulations to verify:

- for the whole structure, its behaviour under the effect of an earthquake and its safety regarding the instability of the arches without transversal bracing. The first two instability load factor are equal to 4.84 and 5.09 versus the SLS loading (Fig. 24).
- for certain structural elements, the effects of the second order effect such as the vertical webs of the steel hollow caissons of the deck for which the phenomenon of web breathing for the common caisson deck-arch at the top of the arches would occurred.

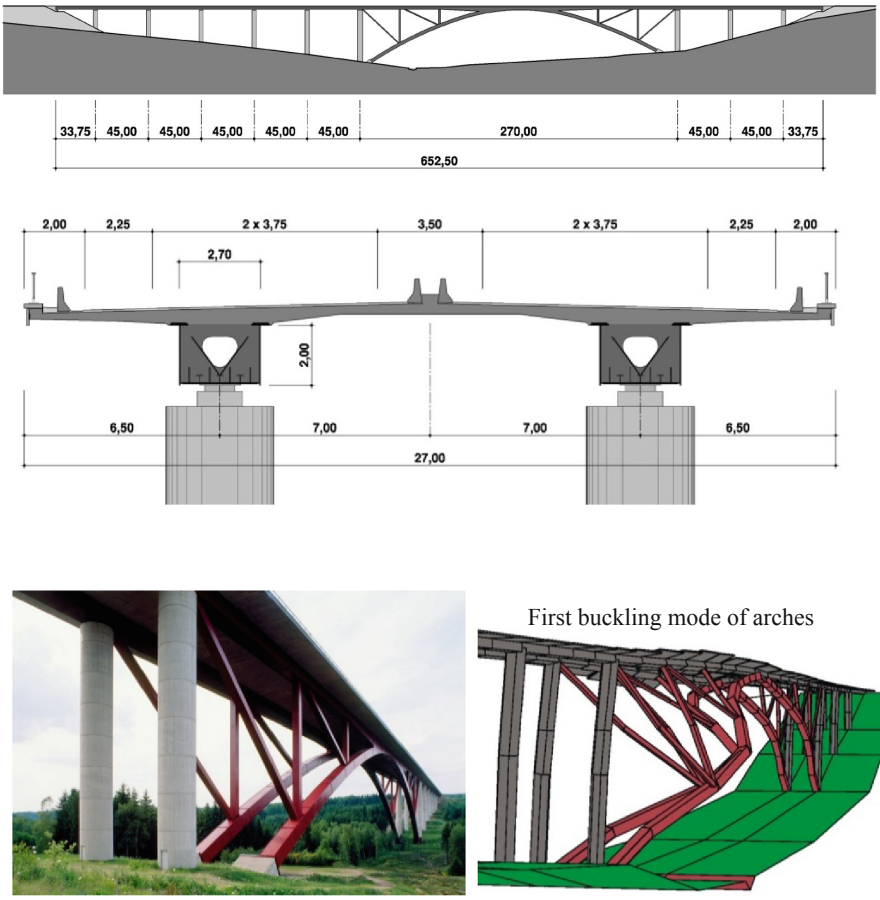

Fig. 24. Eau-Rouge Viaduct

5.2 Bridge on the Ravine Fontaine

The arch bridge on the Ravine Fontaine (Fig. 25) is a bridge on the road connection called "Route des Tamarins" in the West of the Reunion Island (France). It is one of the four civil engineering works qualified as exceptional on this road because of their type, their dimensions and/or their location. The Tamarins road progresses on the sides of a volcano, approximately one km away from the coast and at an altitude close to 300 m. It must consequently cross the innumerable ravines. The Ravine Fontaine has at the level of the road, an opening of 200 m and a depth of 110 m. The deck is 20.1 m width: 2 road lanes and an emergency lane in each direction [8].

As first approach, it was reasonable to consider (Fig. 25) [9]:

- for a bridge whose reactions would have been vertical, that the support zone must lie a setback of 20 m relative to the edge of the cliffs and find a basalt layer sufficiently thick to allow diffusion of the support reactions
- for a bridge with inclined reactions (arch type bridge), that it was necessary to consider the zone following the natural balancing slope as unstable, and that a support surface directly behind this zone was acceptable, as far as it was possible to find one or more basalt layers which were able to balance the horizontal component.

The Reunion island is the seat of a very significant endemic flora of which many species are protected. In particular, certain birds such as the "puffins of the baillon`` nest and reproduce in the cracks and fractures of the basalt layers. It was not possible to envisage a cable-stayed bridge that would have disrupted their flight.

In consequence, the best choice was a bridge with a support structure below the deck: an arch bridge. The length of the structure is strictly limited to what is needed for carrying out the crossing, this is 200 m. It is easily understood that if the geotechnical conditions allow the construction of an arch bridge, this solution will be the most interesting, as much as well as for the landscape, as technical and economic aspects.

The principle of an arch bridge is such that it is principally subjected to an almost constant compression force. It is therefore logical to design a constant section. The design takes account of this principle. However, to benefit from the possibilities of restraining the arch in the foundations and in the basalt layers, the height of the section was increased at the basis, which also made it possible to decrease it in the central part and to give the impression of a large slenderness. Transversely, the arch is mainly subjected to the forces of the wind (mean wind speed, 50 m/sec, in cyclone regions). It behaves like a beam supported at its two ends, with a maximum bending moment in the central part. The width of its section develops proportionally to this bending moment. These principles have made it possible to fit the arch section between two inclined planes (Fig. 26).

The geometry of the arch so defined was used as the basis for the geometrical construction of the columns and the deck. The deck is composed of two small caissons 2 m high and 2 m wide. These two small caissons are braced every 4 m in order to support the reinforced concrete slabs. They are in addition supported by the radiating, thus inclined columns. The columns as well as the caissons of the deck fit in the planes of the arch.

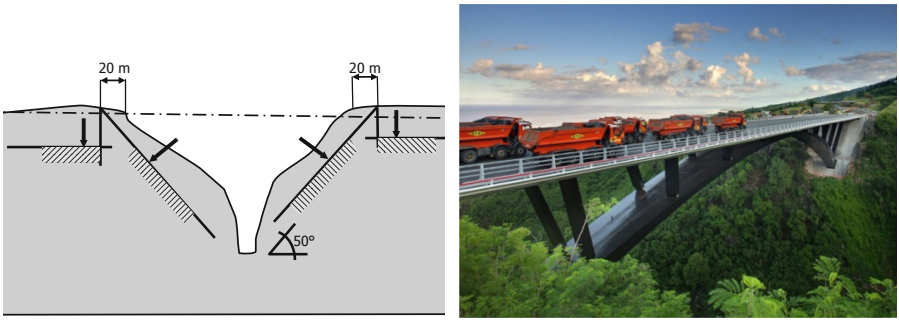

Fig. 25. Ravine Fontaine profile and the bridge.

The ratio L/f, height of the arch on span length, is usually guided by economic considerations and lies between 5 and 6 (see tied arch bridges on the Albert Canal). In addition, with the general rule, other parameters have to be considered. The foundations must find a sufficiently rigid support on the basalt layers to take the compression of the arch. The abrupt face of the cliffs makes the earthworks and the access to the bottom of the excavation particularly delicate. It is necessary to limit their depth to the minimum. But aesthetically, the economic ratio leads to a less dynamic aspect. This is why we made the choice to decrease the slenderness ratio to 1/7.5, that is a deflection of 22.50 m for a span of 170 m.

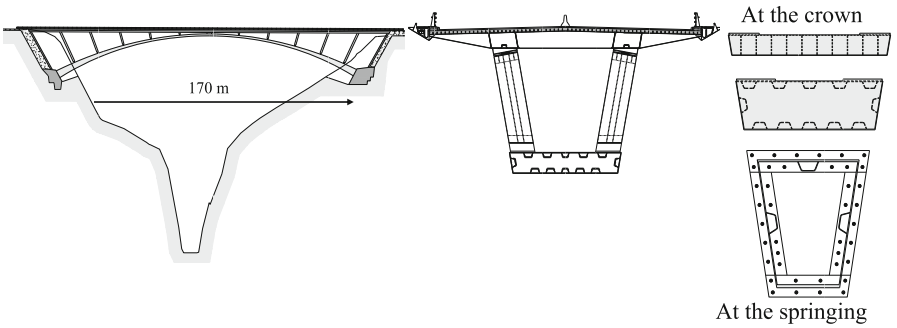

Fig. 26. Bridge on Ravine Fontaine – Elevation and cross sections

The four sides of the box girder consist of stiffened panels (Fig. 26). These panels were checked by means of Eurocode by taking account of the combined plate-column behaviour.

Two by two and laid out every 16 m, the columns transfer the loads coming from the deck onto the arch. They are provided with articulations at their two ends in order to be subjected only to normal forces. Indeed, under the effect of the asymmetrical forces (a longitudinally loaded half-bridge), the arch works exclusively in bending and significantly deforms, inducing significant relative rotations, particularly at the foot of the

columns. An end restraint at this place would have imposed a bending of the columns incompatible with their resistance to fatigue. In order to ensure this function and to limit the maintenance (inspection, replacement), the supports at the interface with the deck are carried out by means of steel grains on steel, and at the arch, by means of a welded plate (Fig. 27).

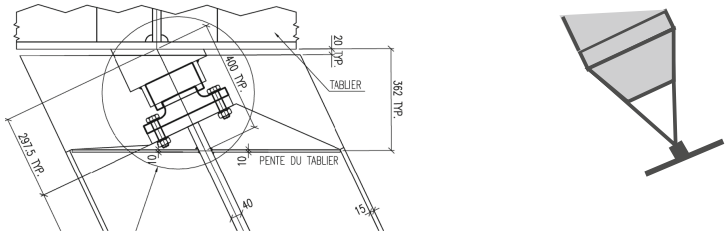

Fig. 27. Interface between counters and the deck and the arch.

After construction of the earthworks, foundations and support abutments, the assembly of the metallic structure, with a total weight of 2000 tons, was erected by the cantilever method (Fig. 28). Basic sections are manufactured in workshops in Italy before being conveyed by boat to the Reunion. After assembly on site to reconstitute elements of a maximum weight of 100 tons, the latter are set up one after the others by means of a derrick built explicitly for this work.

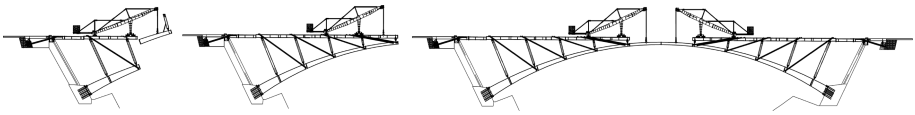

Fig. 28. Erection stages of the steel structure

6 Conclusions

Although numerous arch and tied-arch bridges have already been designed around the world, it is yet possible to imagine innovative structures. But, the most important thing is perhaps to design aesthetic and elegant structures with the respect of their environment.

The beliefs of René Greisch about appropriateness of design in relation to efficiency, economy and functionality have been expressed in a series of works which have established the reputation and the references of his engineering office. His interest in architecture has instilled his design team with a spirit of research and innovation and has led to many collaboration ventures with architects. Collaboration between engineers and architects is important in order to create an atmosphere where the design team is constantly questioning and searching for new solutions, both formal and technical. The attitude of quest, the determination to work through collaboration and

synergy, constant innovation and dynamism, invention combined with imagination must become the working methods and principles that must underpin the design of structures and bridges.

The bridges must be designed to serve the city with the respect of three well-known principles: the statics, the aesthetics and the politics.

Then, there will be many chances that citizens will be proud of "their" bridges.

References

1. de Ville de Goyet, V., Fonder, Gh., Lothaire, A.: Stability of a bowstring bridge with twin inclined arches. In: Proceedings of IABSE Workshop "lnformatics in Structural Engineering", Bergamo (1982)
2. de Ville de Goyet, V.: L'analyse statique non linéaire par la méthode des éléments finis des structures spatiales formées de poutres à section non symé trique, Ph.D., Department MSM. University of Liege, Belgium (1988)
3. de Ville de Goyet, V., Massonnet, C.E.: Comparative Study of the Stability of Various Dispositions of Tied Arch Bridges, Der Stallbau in Konstruktiven - Ingenieurbau Festive, Publication for Professor BAEHRE, Karlsruhe (1988)
4. Ney, L., de Ville de Goyet, V., Maquoi, R.: Optimum bracing of the arches of tied-arch bridges. J. Constr. Steel Res. **18**, 239–249 (1991)
5. Dubas, P., Gehri, E.: Behaviour and Design of Steel Plated Structures. ECCS, no. 44 (1986)
6. Jacques, Th., Maquoi, R., Fonder, G.: Buckling of unstiffened compression curved plates. J. Constr. Steel Res. **3**, 28–34 (1983)
7. de Ville de Goyet, V.: Illustration of Design Constraints for Composite Railway Viaducts with Some Recent Structures, Associacon Cientifico-tecnica del Hormigon Estructural, Madrid (2009)
8. Cremer, J.-M., de Ville de Goyet, V., Lothaire, A., Radu, V.: Viaduc de l'eau rouge, études spéciales, Construction Métallique, no. 1 (1994)
9. Cremer, J.-M., Del Forno, J.-Y., Klein, J.-F.: The bridge over the ravine "la fontaine", Reunion Island. In: Proceedings of 7th International Conference on Steel Bridges, Guimaraes, Portugal (2008)

Challenge and Development of Long Span Arch Bridges in Statics, Dynamics and Aerodynamics

Yaojun Ge(✉)

Tongji University, Shanghai 200092, China
yaojunge@tongji.edu.cn

Abstract. As one of the most formidable challenges on long-span bridges, recent development of arch bridges have been presented in the aspects of static stability, dynamic characteristics and aerodynamic performance. Concrete, steel and concrete-filled-steel-tube arch bridges have been numerically analyzed to evaluate elastic structural buckling instability and plastic material yielding instability. Concrete arch bridges may result in plastic material yielding instability during construction, especially under strong winds, although completed bridges have quite high safety factor. Most long span bridges show good dynamic characteristics, and have higher structural stiffness and natural frequency than those of cable-stayed bridges with same span length. Steel box rib arch bridges have been found with some aerodynamic problems due to very bluff cross section, especially in vortex-induced vibration, but the increase in span length of arch bridges should not be influenced by aerodynamic performance.

Keywords: Arch bridge · Statics · Dynamics · Aerodynamics

1 Introduction

Human beings have been building bridges in girder, arch, cable-stayed and suspension types in order to cross streams and rivers for thousands of years. Arch bridge is an ancient bridge type originating from stone arch, which was firstly invented around 2,500 BC in the ancient Greeks, and developed most fully for arch bridges by the ancient Romans. China has an ancient history of arch bridge construction for about 2,000 years, and the oldest existing bridge is Zhaozhou Bridge of 605 AD, which is the world's first wholly-stone open-spandrel segmental arch bridge. In the modern time of 1930's, two famous long-span steel arch bridges were completed, namely the 504 m Bayonne Bridge in the United States and the 503 m Sydney Harbour Bridge in Australia, which remained to be the longest arches for about four decades, till the emergence of 518 m New River Gorge Bridge of USA in 1977. After another four decades, China has built several remarkable arch bridges with very long spans, including two world record-breaking spans of 550 m Lupu Bridge in Shanghai and 552 m Chaotianmen Bridge in Chongqing. The top ten longest span steel arch bridges in the world are listed in Table 1 [1].

A. Arêde and C. Costa (Eds.): ARCH 2019, SI 11, pp. 71–91, 2020.
https://doi.org/10.1007/978-3-030-29227-0_4

Table 1. Top ten longest span steel arch bridges.

No.	Bridge name	Span(m)	Arch rib	Country	Built year
1	Chaotianmen Bridge	552	Truss	China	2009
2	Lupu Bridge	550	Box	China	2003
3	New River Gorge Bridge	518	Truss	USA	1977
4	Bayonne Bridge	510	Truss	USA	1931
5	Sydney Harbour Bridge	503	Truss	Australia	1932
6	Mingzhou Bridge	450	Box	China	2011
7	Zhaoqing Xijiang Bridge	450	Box	China	2013
8	Xinguang Bridge	428	Box	China	2008
9	Caiyuanba Bridge	420	Box	China	2007
10	Second Hengqin Bridge	400	Truss	China	2015

In addition to steel, concrete is another structural material that can also be used in arch bridge construction since arches are mainly subjected to compressive forces. There are many concrete arch bridges with long spans, and the top ten in the world are shown in Table 2 [2].

Table 2. Top ten longest span concrete arch bridges.

No.	Bridge name	Span(m)	Arch rib	Country	Built year
1	Beipan River Bridge	450	Concrete	China	2016
2	Wanxian Bridge	420	Concrete	China	1997
3	Krk Bridge	416	Concrete	Croatia	1980
4	Nanpan River Bridge	416	Concrete	China	2016
5	Almonte River Railway Br.	384	Concrete	Spain	2016
6	Zhaohua Jialing River Bridge	364	Concrete	China	2012
7	Jiangjiehe Bridge	330	Concrete	China	1993
8	Mike O'Callaghan-Pat Tillman Memorial Bridge	323	Concrete	USA	2010
9	Yongjiang Bridge	312	Concrete	China	1996
10	Gladesville Bridge	305	Concrete	Australia	1964

As steel and concrete composite structure, concrete filled in steel tube (CFST) has been used in arch ribs of long-span arch bridges, and CFST arch rib bridge construction began with Russia, followed by Japan, and widely developed in China. Due to the construction cost and duration, over 400 CFST arch bridges have already been built in China. Table 3 lists the top ten longest span CFST arch bridges in the world, all of which are in China [2].

Table 3. Top ten longest span CFST arch bridges.

No.	Bridge name	Span(m)	Arch rib	Country	Built year
1	Bosideng Bridge	530	CFST	China	2012
2	Wushan Bridge	460	CFST	China	2005
3	Zhijinghe Bridge	430	CFST	China	2009
4	Lianxiang Bridge	400	CFST	China	2007
5	Daninghe Bridge	400	CFST	China	2010
6	Maocaojie Bridge	368	CFST	China	2006
7	Yajisha Bridge	360	CFST	China	2000
8	Zongqihe Bridge	360	CFST	China	2015
9	Zhunshuo Railway Bridge	357	CFST	China	2018
10	Xiaohe River Bridge	338	CFST	China	2010

With the increase of arch bridge span length, arch bridges are becoming more flexible, which requires to investigate static stability, dynamic characteristics and aerodynamic performance. The analysis of static stability has been carried out on concrete, steel and CFST arch bridges to evaluate their elastic structural buckling instability and plastic material yielding instability. Dynamic characteristics analysis with finite element method (FEM) has been conducted on several long-span arch bridges, and the natural frequencies of these bridges have been compared with those of cable-stayed bridges. Considering aerodynamic performance of long span arch bridges, Shanghai Lupu Bridge has been systematically investigated on vortex-induced vibration.

2 Static Stability of Concrete, Steel and CFST Arch Bridges

Arch ribs are main force-bearing members of arch bridges. They are generally in an eccentric compression state under static load and face the challenge of structural static stability. The static stability analysis needs to consider not only vertical structural dead load and live vehicle load but also static wind loads including vertical static wind lift, lateral wind drag and torsional wind moment. Long-span arch bridges do not need to consider vehicle loads under extreme static wind loads since the deck traffic may close in that time, but static instability may still occur.

The static instability of arch bridges is generally divided into elastic structural buckling instability (the first type of instability) and plastic material yielding instability (the second type of instability). In the elastic structural buckling instability, static load relies on structural deformation obviously and the load can be linear or nonlinear. The static wind load produces a so-called aerodynamic stiffness (also known as load stiffness). Due to the contribution of aerodynamic stiffness, the geometric stiffness can be negative, and the compressed arch bridge system may lose its overall stability. The mechanism of the second type of instability is different from the first one. It occurs when structural effects of dead load, live load and static wind load are beyond the ultimate bearing capacity of the arch bridge. Contribution of negative aerodynamic

stiffness still cannot be ignored and nonlinear structure performance is also very important in this type of instability [1].

Three arch bridges respectively with concrete, steel and CFST ribs have been taken as examples to analyze their static stability, and the corresponding results are presented below.

2.1 Reinforced Concrete Arch Bridge

Linking Yibin City and Zigong City over the Min River in Sichuan Province, the 2nd Yibin Bridge is a three-span continuous reinforced concrete (RC) arch bridge with the equal span length of 160 m, as shown in Fig. 1. The load-bearing main arch consists of ten RC box-arch-ribs, 1.6 m wide and 2.2 m deep each, which are segmentally erected with the sequence of one box rib by one box rib without any temporary supporters. After two RC box ribs with the cross section show in Fig. 2 had been constructed through all three spans, the central span and the side span near Zigong City were found to have collapsed into the river during the night of June 6, 1997. The construction work was stopped afterwards in order to investigate the accident. Unfortunately, the remaining side span near Yibin City was collapsed again on August 29, 1997.

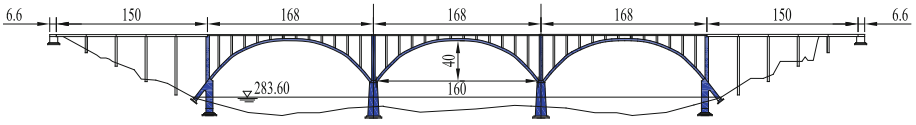

Fig. 1. General arrangement of the 2nd Yibin Bridge

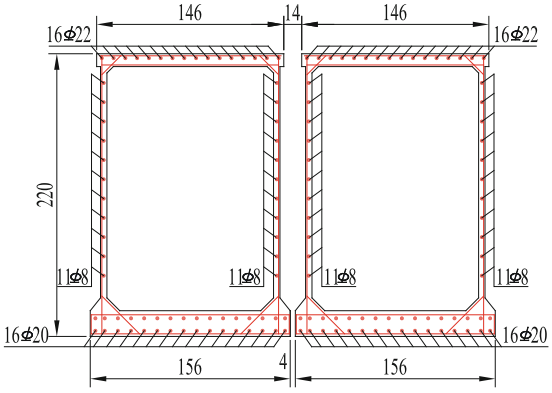

Fig. 2. The cross section of two RC box ribs erected

In order to investigate the collapse of the 2nd Yibin Bridge under construction, theoretical analysis and wind tunnel tests were conducted, and static instabilities due to

static wind loading and dynamic wind loading were analyzed. Finally, the reason for the collapse of the arch ribs was concluded [3].

Static Stability due to Static Wind Loading

Static wind loading or aerostatic force can be divided into three components, drag force F_D or horizontal force F_H, lift force F_L or vertical force F_N and pitching moment M_T, and can be defined in the following equations and Fig. 3.

$$F_D = \frac{1}{2}\rho U^2 H C_D \text{ or } F_H = \frac{1}{2}\rho U^2 H C_H \tag{1}$$

$$F_L = \frac{1}{2}\rho U^2 B C_L \text{ or } F_N = \frac{1}{2}\rho U^2 B C_N \tag{2}$$

$$M_L = \frac{1}{2}\rho U^2 B^2 C_M \tag{3}$$

where ρ is air mass density, ρ = 1.225 kg/m^3; U is mean wind speed, U = 29 m/s at the arch crown level of 60 m; B is section width, B = 3.2 m; H is section height, H = 2.2 m; C_D and C_H are aerostatic drag and horizontal coefficients respectively; C_L and C_N are aerostatic lift and vertical coefficients respectively; and C_M is aerodynamic pitching moment coefficient. The aerostatic force coefficients defined in Eqs. (1)–(3) were identified through the sectional model force balance testing shown in Fig. 4.

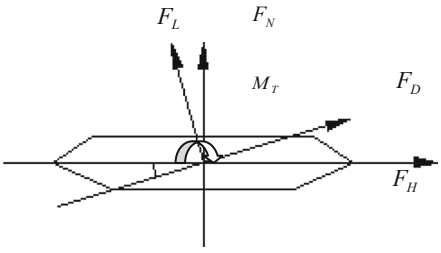

Fig. 3. Aerostatic force components

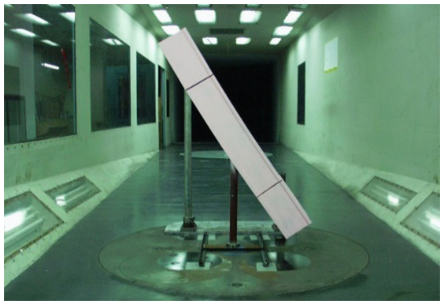

Fig. 4. Sectional model force balance testing

According to the definition of aerostatic forces in Eqs. (1)–(3), the three components of aerostatic loads can be expressed by

$$W^s_{y,z,\theta}(x) = \overline{W}_{y,z,\theta}\alpha_{y,z,\theta}(x) \tag{4}$$

where $\overline{W}_{y,z,\theta}$ is the maximum values of aerostatic loads; $\alpha_{y,z,\theta}(x)$ is the non-dimensional distribution functions of aerostatic loads; y is for horizontal direction; z is for vertical direction; and θ is for pitch direction. The mean wind speed during construction stage can be calculated by

$$U_z^s = U_d^s \left(\frac{z}{z_d}\right)^{\alpha} = 29.0 \times \left(\frac{z}{z_d}\right)^{0.16} \tag{5}$$

where z is height above the water; and $\alpha = 0.16$. Therefore, the non-dimensional distribution functions of aerostatic loads are expressed as

$$\alpha_y(x) = \alpha_\theta(x) = \left(\frac{z}{z_d}\right)^{2\alpha} = \left(\frac{\frac{4x^2}{l^2} + \frac{h_0}{f}}{1 + \frac{h_0}{f}}\right)^{2\alpha} = \left(1 - 0.673\frac{x^2}{4l^2}\right)^{0.32} \tag{6}$$

$$\alpha_z(x) = \left(\frac{z}{z_d}\right)^{2\alpha} \cdot \cos\beta \approx (1 - 0.673\frac{x}{4l^2})^{0.32} \cdot \cos\frac{\pi}{2l}x \tag{7}$$

The maximum values of aerostatic loads during construction stage are

$$\overline{W}_y = \frac{1}{2}\rho U^2 H C_H = 1.53 \text{ kN/m} \tag{8}$$

$$\overline{W}_z = \frac{1}{2}\rho U^2 B C_N = -0.0609 \text{ kN/m} \tag{9}$$

$$\overline{W}_\theta = \frac{1}{2}\rho U^2 B^2 C_M = 0.0866 \text{ kN-m/m} \tag{10}$$

Based on the dead load of arch ribs under construction and the aerostatic loads described in Eq. (4), the incremental iteration method was used to analyze static stability on the three dimensional finite element method (FEM) model of the arch ribs. The vertical and horizontal displacements at mid-span and quarter-span are shown in Fig. 5 with the wind speed increment of 10 m/s. It can be concluded that the structural static instability does not happen until the maximum wind speed of 150 m/s.

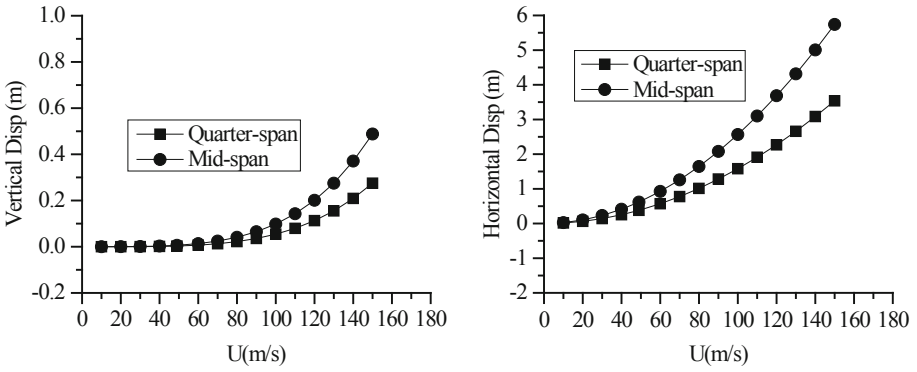

Fig. 5. Vertical and horizontal displacements

Static Stability due to Dynamic Wind Loading

Since static wind loading does not include the force due to wind-induced structural vibration, dynamic wind loading is defined with aerodynamic and aeroelastic responses of a structure. For simplicity in static stability calculation, dynamic wind loading is usually transferred to equivalent aerostatic loading, which is defined in the condition that the displacements of bridge structures under this equivalent aerostatic loading are equal to the maximum oscillation displacements. The equivalent aerostatic loading on arch ribs can be determined by

$$W_{y,z,\theta} = g_{W_{y,z,\theta}} \sigma_{W_{y,z,\theta}} = g_{W_{y,z,\theta}} \sqrt{\sigma^2_{W_{b\,y,z,\theta}} + \sigma^2_{W_{r\,y,z,\theta}}} = g_{W_{y,z,\theta}} \sqrt{1 + \mu_{y,z,\theta}} \sigma_{W_{r\,y,z,\theta}} \tag{11}$$

where g_w is peak factor; μ is modification factor due to background response; and σ_w is root-mean-square (RMS) of resonant response due to dynamic wind loading.

The most accurate method in determining the above-mentioned three parameters, peak factor, modification factor and RMS, is wind tunnel testing with a full aeroelastic model. Based on the experimental results of the aeroelastic model testing in Fig. 6, the equivalent aerostatic loading of the arch ribs can be expressed by the following expressions and Fig. 7.

$$W_y(x) = (1 - 0.673\frac{x^2}{4l^2})^{0.32}(1.53 \pm 0.75\cos\frac{\pi}{l}x \pm 0.55\sin\frac{2\pi}{l}x) \tag{12}$$

$$W_z(x) = (1 - 0.673\frac{x^2}{4l^2})^{0.32}(-0.0609 \pm 0.80\cos\frac{3\pi}{l}x \pm 2.10\sin\frac{2\pi}{l}x) \cdot \cos\frac{\pi}{2l}x \tag{13}$$

$$W_\theta(x) = (1 - 0.673\frac{x^2}{4l^2})^{0.32}(0.0866 \pm 0.50\cos\frac{\pi}{l}x \pm 0.40\sin\frac{2\pi}{l}x) \tag{14}$$

Fig. 6. Full-scale aeroelastic model testing

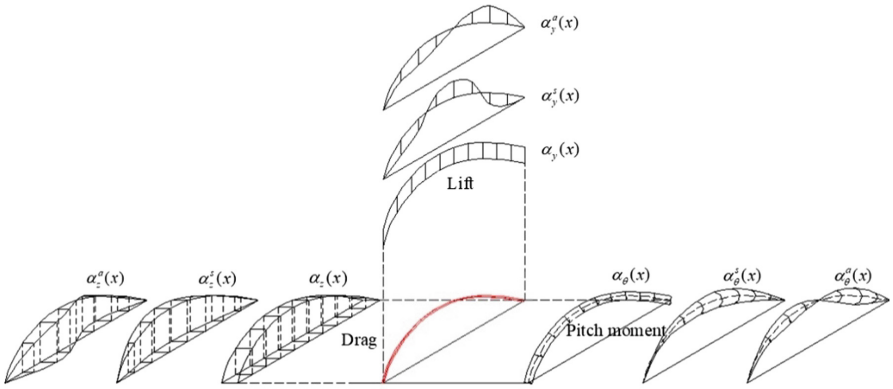

Fig. 7. Equivalent aerostatic loading

The dead load on the arch rib can be defined as

$$q_z = m \cdot g = 35.45 \text{ kN/m} \tag{15}$$

The internal forces at different cross sections caused by the dead load, the aerostatic loading and the equivalent aerostatic loading were calculated, and the influence of P-Δ effect was also considered. The RC rib strength evaluation is conducted with the condition that the axial force N_p based on the load combinations is equal to the structural ultimate resistance N_R.

At the arch crown cross section, when $N_p = N_R = 3390$ kN, the structural in-plain resistant bending moment $M_R = 24086$ kN-m is much greater than the value of $M_p = 487.3$ kN-m due to the code or the value of $M_p = 848.7$ kN-m due to the wind tunnel tests, and the structural out-of-plain resistant bending moment $M_R = 4234$ kN-m is greater than the value of $M_p = 2324$ kN due to the code but much than the value of $M_p = 6612$ kN due to the wind tunnel tests. Similarly, at the arch foot cross section, when $N_p = N_R = 4963$ kN, the structural in-plain resistant bending moment $M_R = 23976$ kN-m is much greater than the value of $M_p = 64.9$ kN-m due to the code but less than the value of $M_p = 497.8$ kN-m due to the wind tunnel tests, and the structural out-of-plain resistant bending moment $M_R = 5534$ kN-m is greater than the value of $M_p = 5192$ kN due to the code but much less than the value of $M_p = 12158$ kN due to the wind tunnel tests. Therefore, the two RC arch ribs of the 2nd Yibin Bridge may fail under the joint action of structural dead loads and wind-induced loads including aerodynamic wind loading, aeroelastic wind loading and the loading based on P-Δ effects which were not considered in the design of the bridge under construction.

2.2 CFST Arch Bridge

CFST is an advanced steel-concrete composite structure with an external steel tube and internal filled plain concrete. The external steel tube works not only as a part of structural material like in reinforced concrete but also to restrain lateral deformation of the internal concrete so that it can behave under three-dimensional compressive state,

which is the most effective, economical and desirable way for concrete. Compared with steel or concrete arch ribs, CFST rib arch bridges can economize steel and concrete consumption and reduce construction costs [4].

As shown in Fig. 8, Xiangshan North Gate Bridge is a basket-type CFST half-through arch bridge with a central span of 270 m. The arch height is 54 m and the ratio of height to span is 1/5. Each arch rib consists of four CFST members with a diameter of 1 m, and these four members are connected by steel pipes, forming a truss arch rib. Two inclined arch ribs are connected by several steel pipe bracings. The bridge girder is made up of prestressed concrete with the deck width of 12.5 m. The first and the second type of instability analysis were carried out based on the FEM model, where steel pipe and internal concrete are individually simulated by different elements. The reference wind speed at the arch crown height is set to be 65 m/s [5].

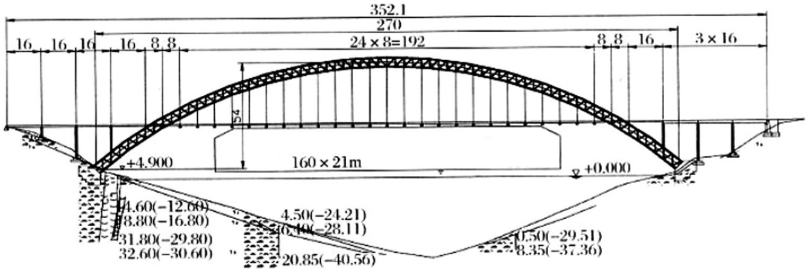

Fig. 8. General arrangement of Xiangshan North Gate Bridge

Elastic Structural Buckling Failure

Since the bridge is closed to traffic when wind speed is beyond a specific limit and no vehicle load is there, the elastic structural buckling failure analysis needs to consider merely structural dead load and static wind load. Assume that in the first iteration wind speed U_1 is 100 m/s, adopt corresponding static wind load and structure dead load to the FEM model, and the first 5 eigen values and the critical wind speed can be determined in Table 4. The first mode of elastic structural buckling failure is shown in Fig. 9. The safety factor for elastic structural buckling failure is determined as 5.896 according to calculation results, which means that there will be elastic structural instability when the total load (structural dead load + static wind load) is expanded by 5.859 times.

Through the second iteration with $U_2 = \sqrt{5.859} \times 100 = 242$ m/s, and the third and the fourth iterations, we can get the result of the first 5 eigen values and the critical wind speeds shown in Table 4. With the fixed value of structural dead load, the safety factor for elastic structural buckling failure is 6.081, which means that there will be elastic structural instability when the static wind load is expanded by 6.081 times [5].